



Measurement of the CKM angle γ from a combination of $B^\pm \rightarrow Dh^\pm$ analyses

The LHCb collaboration[†]

Abstract

A combination of three LHCb measurements of the CKM angle γ is presented. The decays $B^\pm \rightarrow DK^\pm$ and $B^\pm \rightarrow D\pi^\pm$ are used, where D denotes an admixture of D^0 and \bar{D}^0 mesons, decaying into K^+K^- , $\pi^+\pi^-$, $K^\pm\pi^\mp$, $K^\pm\pi^\mp\pi^\pm\pi^\mp$, $K_S^0\pi^+\pi^-$, or $K_S^0K^+K^-$ final states. All measurements use a dataset corresponding to 1.0 fb^{-1} of integrated luminosity. Combining results from $B^\pm \rightarrow DK^\pm$ decays alone a best-fit value of $\gamma = 72.0^\circ$ is found, and confidence intervals are set

$$\gamma \in [56.4, 86.7]^\circ \quad \text{at 68\% CL,}$$

$$\gamma \in [42.6, 99.6]^\circ \quad \text{at 95\% CL.}$$

The best-fit value of γ found from a combination of results from $B^\pm \rightarrow D\pi^\pm$ decays alone, is $\gamma = 18.9^\circ$, and the confidence intervals

$$\gamma \in [7.4, 99.2]^\circ \cup [167.9, 176.4]^\circ \quad \text{at 68\% CL}$$

are set, without constraint at 95% CL. The combination of results from $B^\pm \rightarrow DK^\pm$ and $B^\pm \rightarrow D\pi^\pm$ decays gives a best-fit value of $\gamma = 72.6^\circ$ and the confidence intervals

$$\gamma \in [55.4, 82.3]^\circ \quad \text{at 68\% CL,}$$

$$\gamma \in [40.2, 92.7]^\circ \quad \text{at 95\% CL}$$

are set. All values are expressed modulo 180° , and are obtained taking into account the effect of $D^0-\bar{D}^0$ mixing.

To be submitted to Phys. Lett. B.

© CERN on behalf of the LHCb collaboration, license CC-BY-3.0.

[†]Authors are listed on the following pages.

LHCb collaboration

R. Aaij⁴⁰, C. Abellan Beteta^{35,n}, B. Adeva³⁶, M. Adinolfi⁴⁵, C. Adrover⁶, A. Affolder⁵¹, Z. Ajaltouni⁵, J. Albrecht⁹, F. Alessio³⁷, M. Alexander⁵⁰, S. Ali⁴⁰, G. Alkhazov²⁹, P. Alvarez Cartelle³⁶, A.A. Alves Jr^{24,37}, S. Amato², S. Amerio²¹, Y. Amhis⁷, L. Anderlini^{17,f}, J. Anderson³⁹, R. Andreassen⁵⁶, R.B. Appleby⁵³, O. Aquines Gutierrez¹⁰, F. Archilli¹⁸, A. Artamonov³⁴, M. Artuso⁵⁸, E. Aslanides⁶, G. Auriemma^{24,m}, S. Bachmann¹¹, J.J. Back⁴⁷, C. Baesso⁵⁹, V. Balagura³⁰, W. Baldini¹⁶, R.J. Barlow⁵³, C. Barschel³⁷, S. Barsuk⁷, W. Barter⁴⁶, Th. Bauer⁴⁰, A. Bay³⁸, J. Beddow⁵⁰, F. Bedeschi²², I. Bediaga¹, S. Belogurov³⁰, K. Belous³⁴, I. Belyaev³⁰, E. Ben-Haim⁸, G. Bencivenni¹⁸, S. Benson⁴⁹, J. Benton⁴⁵, A. Berezhnoy³¹, R. Bernet³⁹, M.-O. Bettler⁴⁶, M. van Beuzekom⁴⁰, A. Bien¹¹, S. Bifani⁴⁴, T. Bird⁵³, A. Bizzeti^{17,h}, P.M. Bjørnstad⁵³, T. Blake³⁷, F. Blanc³⁸, J. Blouw¹¹, S. Blusk⁵⁸, V. Bocci²⁴, A. Bondar³³, N. Bondar²⁹, W. Bonivento¹⁵, S. Borghi⁵³, A. Borgia⁵⁸, T.J.V. Bowcock⁵¹, E. Bowen³⁹, C. Bozzi¹⁶, T. Brambach⁹, J. van den Brand⁴¹, J. Bressieux³⁸, D. Brett⁵³, M. Britsch¹⁰, T. Britton⁵⁸, N.H. Brook⁴⁵, H. Brown⁵¹, I. Burducea²⁸, A. Bursche³⁹, G. Busetto^{21,p}, J. Buytaert³⁷, S. Cadeddu¹⁵, O. Callot⁷, M. Calvi^{20,j}, M. Calvo Gomez^{35,n}, A. Camboni³⁵, P. Campana^{18,37}, D. Campora Perez³⁷, A. Carbone^{14,c}, G. Carboni^{23,k}, R. Cardinale^{19,i}, A. Cardini¹⁵, H. Carranza-Mejia⁴⁹, L. Carson⁵², K. Carvalho Akiba², G. Casse⁵¹, L. Castillo Garcia³⁷, M. Cattaneo³⁷, Ch. Cauter⁹, M. Charles⁵⁴, Ph. Charpentier³⁷, P. Chen^{3,38}, N. Chiapolini³⁹, M. Chrzaszcz³⁹, K. Ciba³⁷, X. Cid Vidal³⁷, G. Ciezarek⁵², P.E.L. Clarke⁴⁹, M. Clemencic³⁷, H.V. Cliff⁴⁶, J. Closier³⁷, C. Coca²⁸, V. Coco⁴⁰, J. Cogan⁶, E. Cogneras⁵, P. Collins³⁷, A. Comerma-Montells³⁵, A. Contu¹⁵, A. Cook⁴⁵, M. Coombes⁴⁵, S. Coquereau⁸, G. Corti³⁷, B. Couturier³⁷, G.A. Cowan⁴⁹, D.C. Craik⁴⁷, S. Cunliffe⁵², R. Currie⁴⁹, C. D'Ambrosio³⁷, P. David⁸, P.N.Y. David⁴⁰, A. Davis⁵⁶, I. De Bonis⁴, K. De Bruyn⁴⁰, S. De Capua⁵³, M. De Cian³⁹, J.M. De Miranda¹, L. De Paula², W. De Silva⁵⁶, P. De Simone¹⁸, D. Decamp⁴, M. Deckenhoff⁹, L. Del Buono⁸, N. Déleage⁴, D. Derkach¹⁴, O. Deschamps⁵, F. Dettori⁴¹, A. Di Canto¹¹, H. Dijkstra³⁷, M. Dogaru²⁸, S. Donleavy⁵¹, F. Dordei¹¹, A. Dosil Suárez³⁶, D. Dossett⁴⁷, A. Dovbnya⁴², F. Dupertuis³⁸, R. Dzhelyadin³⁴, A. Dziurda²⁵, A. Dzyuba²⁹, S. Easo^{48,37}, U. Egede⁵², V. Egorychev³⁰, S. Eidelman³³, D. van Eijk⁴⁰, S. Eisenhardt⁴⁹, U. Eitschberger⁹, R. Ekelhof⁹, L. Eklund^{50,37}, I. El Rifai⁵, Ch. Elsasser³⁹, D. Elsby⁴⁴, A. Falabella^{14,e}, C. Färber¹¹, G. Fardell⁴⁹, C. Farinelli⁴⁰, S. Farry⁵¹, V. Fave³⁸, D. Ferguson⁴⁹, V. Fernandez Albor³⁶, F. Ferreira Rodrigues¹, M. Ferro-Luzzi³⁷, S. Filippov³², M. Fiore¹⁶, C. Fitzpatrick³⁷, M. Fontana¹⁰, F. Fontanelli^{19,i}, R. Forty³⁷, O. Francisco², M. Frank³⁷, C. Frei³⁷, M. Frosini^{17,f}, S. Furcas²⁰, E. Furfaro^{23,k}, A. Gallas Torreira³⁶, D. Galli^{14,c}, M. Gandelman², P. Gandini⁵⁸, Y. Gao³, J. Garofoli⁵⁸, P. Garosi⁵³, J. Garra Tico⁴⁶, L. Garrido³⁵, C. Gaspar³⁷, R. Gauld⁵⁴, E. Gersabeck¹¹, M. Gersabeck⁵³, T. Gershon^{47,37}, Ph. Ghez⁴, V. Gibson⁴⁶, V.V. Gligorov³⁷, C. Göbel⁵⁹, D. Golubkov³⁰, A. Golutvin^{52,30,37}, A. Gomes², H. Gordon⁵⁴, M. Grabalosa Gándara⁵, R. Graciani Diaz³⁵, L.A. Granado Cardoso³⁷, E. Graugés³⁵, G. Graziani¹⁷, A. Grecu²⁸, E. Greening⁵⁴, S. Gregson⁴⁶, P. Griffith⁴⁴, O. Grünberg⁶⁰, B. Gui⁵⁸, E. Gushchin³², Yu. Guz^{34,37}, T. Gys³⁷, C. Hadjivasiliou⁵⁸, G. Haefeli³⁸, C. Haen³⁷, S.C. Haines⁴⁶, S. Hall⁵², T. Hampson⁴⁵, S. Hansmann-Menzemer¹¹, N. Harnew⁵⁴, S.T. Harnew⁴⁵, J. Harrison⁵³, T. Hartmann⁶⁰, J. He³⁷, V. Heijne⁴⁰, K. Hennessy⁵¹, P. Henrard⁵, J.A. Hernando Morata³⁶, E. van Herwijnen³⁷, A. Hicheur¹, E. Hicks⁵¹, D. Hill⁵⁴, M. Hoballah⁵, C. Hombach⁵³, P. Hopchev⁴, W. Hulsbergen⁴⁰, P. Hunt⁵⁴, T. Huse⁵¹, N. Hussain⁵⁴, D. Hutchcroft⁵¹, D. Hynds⁵⁰, V. Iakovenko⁴³, M. Idzik²⁶, P. Ilten¹², R. Jacobsson³⁷, A. Jaeger¹¹, E. Jans⁴⁰, P. Jaton³⁸, A. Jawahery⁵⁷, F. Jing³,

M. John⁵⁴, D. Johnson⁵⁴, C.R. Jones⁴⁶, C. Joram³⁷, B. Jost³⁷, M. Kaballo⁹, S. Kandybei⁴²,
M. Karacson³⁷, T.M. Karbach³⁷, I.R. Kenyon⁴⁴, U. Kerzel³⁷, T. Ketel⁴¹, A. Keune³⁸,
B. Khanji²⁰, O. Kochebina⁷, I. Komarov³⁸, R.F. Koopman⁴¹, P. Koppenburg⁴⁰, M. Korolev³¹,
A. Kozlinskiy⁴⁰, L. Kravchuk³², K. Kreplin¹¹, M. Kreps⁴⁷, G. Krocker¹¹, P. Krokovny³³,
F. Kruse⁹, M. Kucharczyk^{20,25,j}, V. Kudryavtsev³³, T. Kvaratskheliya^{30,37}, V.N. La Thi³⁸,
D. Lacarrere³⁷, G. Lafferty⁵³, A. Lai¹⁵, D. Lambert⁴⁹, R.W. Lambert⁴¹, E. Lanciotti³⁷,
G. Lanfranchi^{18,37}, C. Langenbruch³⁷, T. Latham⁴⁷, C. Lazzeroni⁴⁴, R. Le Gac⁶,
J. van Leerdam⁴⁰, J.-P. Lees⁴, R. Lefèvre⁵, A. Leflat³¹, J. Lefrançois⁷, S. Leo²², O. Leroy⁶,
T. Lesiak²⁵, B. Leverington¹¹, Y. Li³, L. Li Gioi⁵, M. Liles⁵¹, R. Lindner³⁷, C. Linn¹¹, B. Liu³,
G. Liu³⁷, S. Lohn³⁷, I. Longstaff⁵⁰, J.H. Lopes², E. Lopez Asamar³⁵, N. Lopez-March³⁸, H. Lu³,
D. Lucchesi^{21,p}, J. Luisier³⁸, H. Luo⁴⁹, F. Machefert⁷, I.V. Machikhiliyan^{4,30}, F. Maciuc²⁸,
O. Maev^{29,37}, S. Malde⁵⁴, G. Manca^{15,d}, G. Mancinelli⁶, U. Marconi¹⁴, R. Märki³⁸, J. Marks¹¹,
G. Martellotti²⁴, A. Martens⁸, A. Martín Sánchez⁷, M. Martinelli⁴⁰, D. Martinez Santos⁴¹,
D. Martins Tostes², A. Massafferri¹, R. Matev³⁷, Z. Mathe³⁷, C. Matteuzzi²⁰, E. Maurice⁶,
A. Mazurov^{16,32,37,e}, B. Mc Skelly⁵¹, J. McCarthy⁴⁴, A. McNab⁵³, R. McNulty¹²,
B. Meadows^{56,54}, F. Meier⁹, M. Meissner¹¹, M. Merk⁴⁰, D.A. Milanes⁸, M.-N. Minard⁴,
J. Molina Rodriguez⁵⁹, S. Monteil⁵, D. Moran⁵³, P. Morawski²⁵, M.J. Morello^{22,r},
R. Mountain⁵⁸, I. Mous⁴⁰, F. Muheim⁴⁹, K. Müller³⁹, R. Muresan²⁸, B. Muryn²⁶, B. Muster³⁸,
P. Naik⁴⁵, T. Nakada³⁸, R. Nandakumar⁴⁸, I. Nasteva¹, M. Needham⁴⁹, N. Neufeld³⁷,
A.D. Nguyen³⁸, T.D. Nguyen³⁸, C. Nguyen-Mau^{38,o}, M. Nicol⁷, V. Niess⁵, R. Niet⁹, N. Nikitin³¹,
T. Nikodem¹¹, A. Nomerotski⁵⁴, A. Novoselov³⁴, A. Oblakowska-Mucha²⁶, V. Obraztsov³⁴,
S. Oggero⁴⁰, S. Ogilvy⁵⁰, O. Okhrimenko⁴³, R. Oldeman^{15,d}, M. Orlandea²⁸,
J.M. Otalora Goicochea², P. Owen⁵², A. Oyanguren³⁵, B.K. Pal⁵⁸, A. Palano^{13,b}, M. Palutan¹⁸,
J. Panman³⁷, A. Papanestis⁴⁸, M. Pappagallo⁵⁰, C. Parkes⁵³, C.J. Parkinson⁵², G. Passaleva¹⁷,
G.D. Patel⁵¹, M. Patel⁵², G.N. Patrick⁴⁸, C. Patrignani^{19,i}, C. Pavel-Nicorescu²⁸,
A. Pazos Alvarez³⁶, A. Pellegrino⁴⁰, G. Penso^{24,l}, M. Pepe Altarelli³⁷, S. Perazzini^{14,c},
D.L. Perego^{20,j}, E. Perez Trigo³⁶, A. Pérez-Calero Yzquierdo³⁵, P. Perret⁵, M. Perrin-Terrin⁶,
G. Pessina²⁰, K. Petridis⁵², A. Petrolini^{19,i}, A. Phan⁵⁸, E. Picatoste Olloqui³⁵, B. Pietrzyk⁴,
T. Pilar⁴⁷, D. Pinci²⁴, S. Playfer⁴⁹, M. Plo Casasus³⁶, F. Polci⁸, G. Polok²⁵, A. Poluektov^{47,33},
E. Polcarpo², A. Popov³⁴, D. Popov¹⁰, B. Popovici²⁸, C. Potterat³⁵, A. Powell⁵⁴,
J. Prisciandaro³⁸, A. Pritchard⁵¹, C. Prouve⁷, V. Pugatch⁴³, A. Puig Navarro³⁸, G. Punzi^{22,q},
W. Qian⁴, J.H. Rademacker⁴⁵, B. Rakotomiaramanana³⁸, M. Rama¹⁸, M.S. Rangel²,
I. Raniuk⁴², N. Rauschmayr³⁷, G. Raven⁴¹, S. Redford⁵⁴, M.M. Reid⁴⁷, A.C. dos Reis¹,
S. Ricciardi⁴⁸, A. Richards⁵², K. Rinnert⁵¹, V. Rives Molina³⁵, D.A. Roa Romero⁵, P. Robbe⁷,
E. Rodrigues⁵³, P. Rodriguez Perez³⁶, S. Roiser³⁷, V. Romanovsky³⁴, A. Romero Vidal³⁶,
J. Rouvinet³⁸, T. Ruf³⁷, F. Ruffini²², H. Ruiz³⁵, P. Ruiz Valls³⁵, G. Sabatino^{24,k},
J.J. Saborido Silva³⁶, N. Sagidova²⁹, P. Sail⁵⁰, B. Saitta^{15,d}, V. Salustino Guimaraes²,
C. Salzmann³⁹, B. Sanmartin Sedes³⁶, M. Sannino^{19,i}, R. Santacesaria²⁴, C. Santamarina Rios³⁶,
E. Santovetti^{23,k}, M. Sapunov⁶, A. Sarti^{18,l}, C. Satriano^{24,m}, A. Satta²³, M. Savrie^{16,e},
D. Savrina^{30,31}, P. Schaack⁵², M. Schiller⁴¹, H. Schindler³⁷, M. Schlupp⁹, M. Schmelling¹⁰,
B. Schmidt³⁷, O. Schneider³⁸, A. Schopper³⁷, M.-H. Schune⁷, R. Schwemmer³⁷, B. Sciascia¹⁸,
A. Sciubba²⁴, M. Seco³⁶, A. Semennikov³⁰, K. Senderowska²⁶, I. Sepp⁵², N. Serra³⁹, J. Serrano⁶,
P. Seyfert¹¹, M. Shapkin³⁴, I. Shapoval^{16,42}, P. Shatalov³⁰, Y. Shcheglov²⁹, T. Shears^{51,37},
L. Shekhtman³³, O. Shevchenko⁴², V. Shevchenko³⁰, A. Shires⁵², R. Silva Coutinho⁴⁷,
T. Skwarnicki⁵⁸, N.A. Smith⁵¹, E. Smith^{54,48}, M. Smith⁵³, M.D. Sokoloff⁵⁶, F.J.P. Soler⁵⁰,
F. Soomro¹⁸, D. Souza⁴⁵, B. Souza De Paula², B. Spaan⁹, A. Sparkes⁴⁹, P. Spradlin⁵⁰,

F. Stagni³⁷, S. Stahl¹¹, O. Steinkamp³⁹, S. Stoica²⁸, S. Stone⁵⁸, B. Storaci³⁹, M. Straticiu²⁸, U. Straumann³⁹, V.K. Subbiah³⁷, L. Sun⁵⁶, S. Swientek⁹, V. Syropoulos⁴¹, M. Szczekowski²⁷, P. Szczypka^{38,37}, T. Szumlak²⁶, S. T'Jampens⁴, M. Teklishyn⁷, E. Teodorescu²⁸, F. Teubert³⁷, C. Thomas⁵⁴, E. Thomas³⁷, J. van Tilburg¹¹, V. Tisserand⁴, M. Tobin³⁸, S. Tolk⁴¹, D. Tonelli³⁷, S. Topp-Joergensen⁵⁴, N. Torr⁵⁴, E. Tournefier^{4,52}, S. Tourneur³⁸, M.T. Tran³⁸, M. Tresch³⁹, A. Tsaregorodtsev⁶, P. Tsopelas⁴⁰, N. Tuning⁴⁰, M. Ubeda Garcia³⁷, A. Ukleja²⁷, D. Urner⁵³, U. Uwer¹¹, V. Vagnoni¹⁴, G. Valenti¹⁴, R. Vazquez Gomez³⁵, P. Vazquez Regueiro³⁶, S. Vecchi¹⁶, J.J. Velthuis⁴⁵, M. Veltri^{17,g}, G. Veneziano³⁸, M. Vesterinen³⁷, B. Viaud⁷, D. Vieira², X. Vilasis-Cardona^{35,n}, A. Vollhardt³⁹, D. Volyanskyy¹⁰, D. Voong⁴⁵, A. Vorobyev²⁹, V. Vorobyev³³, C. Voß⁶⁰, H. Voss¹⁰, R. Waldi⁶⁰, R. Wallace¹², S. Wandernoth¹¹, J. Wang⁵⁸, D.R. Ward⁴⁶, N.K. Watson⁴⁴, A.D. Webber⁵³, D. Websdale⁵², M. Whitehead⁴⁷, J. Wicht³⁷, J. Wiechczynski²⁵, D. Wiedner¹¹, L. Wiggers⁴⁰, G. Wilkinson⁵⁴, M.P. Williams^{47,48}, M. Williams⁵⁵, F.F. Wilson⁴⁸, J. Wishahi⁹, M. Witek²⁵, S.A. Wotton⁴⁶, S. Wright⁴⁶, S. Wu³, K. Wyllie³⁷, Y. Xie^{49,37}, Z. Xing⁵⁸, Z. Yang³, R. Young⁴⁹, X. Yuan³, O. Yushchenko³⁴, M. Zangoli¹⁴, M. Zavertyaev^{10,a}, F. Zhang³, L. Zhang⁵⁸, W.C. Zhang¹², Y. Zhang³, A. Zhelezov¹¹, A. Zhokhov³⁰, L. Zhong³, A. Zvyagin³⁷.

¹Centro Brasileiro de Pesquisas Físicas (CBPF), Rio de Janeiro, Brazil

²Universidade Federal do Rio de Janeiro (UFRJ), Rio de Janeiro, Brazil

³Center for High Energy Physics, Tsinghua University, Beijing, China

⁴LAPP, Université de Savoie, CNRS/IN2P3, Annecy-Le-Vieux, France

⁵Clermont Université, Université Blaise Pascal, CNRS/IN2P3, LPC, Clermont-Ferrand, France

⁶CPPM, Aix-Marseille Université, CNRS/IN2P3, Marseille, France

⁷LAL, Université Paris-Sud, CNRS/IN2P3, Orsay, France

⁸LPNHE, Université Pierre et Marie Curie, Université Paris Diderot, CNRS/IN2P3, Paris, France

⁹Fakultät Physik, Technische Universität Dortmund, Dortmund, Germany

¹⁰Max-Planck-Institut für Kernphysik (MPIK), Heidelberg, Germany

¹¹Physikalisches Institut, Ruprecht-Karls-Universität Heidelberg, Heidelberg, Germany

¹²School of Physics, University College Dublin, Dublin, Ireland

¹³Sezione INFN di Bari, Bari, Italy

¹⁴Sezione INFN di Bologna, Bologna, Italy

¹⁵Sezione INFN di Cagliari, Cagliari, Italy

¹⁶Sezione INFN di Ferrara, Ferrara, Italy

¹⁷Sezione INFN di Firenze, Firenze, Italy

¹⁸Laboratori Nazionali dell'INFN di Frascati, Frascati, Italy

¹⁹Sezione INFN di Genova, Genova, Italy

²⁰Sezione INFN di Milano Bicocca, Milano, Italy

²¹Sezione INFN di Padova, Padova, Italy

²²Sezione INFN di Pisa, Pisa, Italy

²³Sezione INFN di Roma Tor Vergata, Roma, Italy

²⁴Sezione INFN di Roma La Sapienza, Roma, Italy

²⁵Henryk Niewodniczanski Institute of Nuclear Physics Polish Academy of Sciences, Kraków, Poland

²⁶AGH - University of Science and Technology, Faculty of Physics and Applied Computer Science, Kraków, Poland

²⁷National Center for Nuclear Research (NCBJ), Warsaw, Poland

²⁸Horia Hulubei National Institute of Physics and Nuclear Engineering, Bucharest-Magurele, Romania

²⁹Petersburg Nuclear Physics Institute (PNPI), Gatchina, Russia

³⁰Institute of Theoretical and Experimental Physics (ITEP), Moscow, Russia

³¹Institute of Nuclear Physics, Moscow State University (SINP MSU), Moscow, Russia

³²Institute for Nuclear Research of the Russian Academy of Sciences (INR RAN), Moscow, Russia

- ³³ *Budker Institute of Nuclear Physics (SB RAS) and Novosibirsk State University, Novosibirsk, Russia*
- ³⁴ *Institute for High Energy Physics (IHEP), Protvino, Russia*
- ³⁵ *Universitat de Barcelona, Barcelona, Spain*
- ³⁶ *Universidad de Santiago de Compostela, Santiago de Compostela, Spain*
- ³⁷ *European Organization for Nuclear Research (CERN), Geneva, Switzerland*
- ³⁸ *Ecole Polytechnique Fédérale de Lausanne (EPFL), Lausanne, Switzerland*
- ³⁹ *Physik-Institut, Universität Zürich, Zürich, Switzerland*
- ⁴⁰ *Nikhef National Institute for Subatomic Physics, Amsterdam, The Netherlands*
- ⁴¹ *Nikhef National Institute for Subatomic Physics and VU University Amsterdam, Amsterdam, The Netherlands*
- ⁴² *NSC Kharkiv Institute of Physics and Technology (NSC KIPT), Kharkiv, Ukraine*
- ⁴³ *Institute for Nuclear Research of the National Academy of Sciences (KINR), Kyiv, Ukraine*
- ⁴⁴ *University of Birmingham, Birmingham, United Kingdom*
- ⁴⁵ *H.H. Wills Physics Laboratory, University of Bristol, Bristol, United Kingdom*
- ⁴⁶ *Cavendish Laboratory, University of Cambridge, Cambridge, United Kingdom*
- ⁴⁷ *Department of Physics, University of Warwick, Coventry, United Kingdom*
- ⁴⁸ *STFC Rutherford Appleton Laboratory, Didcot, United Kingdom*
- ⁴⁹ *School of Physics and Astronomy, University of Edinburgh, Edinburgh, United Kingdom*
- ⁵⁰ *School of Physics and Astronomy, University of Glasgow, Glasgow, United Kingdom*
- ⁵¹ *Oliver Lodge Laboratory, University of Liverpool, Liverpool, United Kingdom*
- ⁵² *Imperial College London, London, United Kingdom*
- ⁵³ *School of Physics and Astronomy, University of Manchester, Manchester, United Kingdom*
- ⁵⁴ *Department of Physics, University of Oxford, Oxford, United Kingdom*
- ⁵⁵ *Massachusetts Institute of Technology, Cambridge, MA, United States*
- ⁵⁶ *University of Cincinnati, Cincinnati, OH, United States*
- ⁵⁷ *University of Maryland, College Park, MD, United States*
- ⁵⁸ *Syracuse University, Syracuse, NY, United States*
- ⁵⁹ *Pontifícia Universidade Católica do Rio de Janeiro (PUC-Rio), Rio de Janeiro, Brazil, associated to ²*
- ⁶⁰ *Institut für Physik, Universität Rostock, Rostock, Germany, associated to ¹¹*

^a *P.N. Lebedev Physical Institute, Russian Academy of Science (LPI RAS), Moscow, Russia*

^b *Università di Bari, Bari, Italy*

^c *Università di Bologna, Bologna, Italy*

^d *Università di Cagliari, Cagliari, Italy*

^e *Università di Ferrara, Ferrara, Italy*

^f *Università di Firenze, Firenze, Italy*

^g *Università di Urbino, Urbino, Italy*

^h *Università di Modena e Reggio Emilia, Modena, Italy*

ⁱ *Università di Genova, Genova, Italy*

^j *Università di Milano Bicocca, Milano, Italy*

^k *Università di Roma Tor Vergata, Roma, Italy*

^l *Università di Roma La Sapienza, Roma, Italy*

^m *Università della Basilicata, Potenza, Italy*

ⁿ *LIFAEELS, La Salle, Universitat Ramon Llull, Barcelona, Spain*

^o *Hanoi University of Science, Hanoi, Viet Nam*

^p *Università di Padova, Padova, Italy*

^q *Università di Pisa, Pisa, Italy*

^r *Scuola Normale Superiore, Pisa, Italy*

1 Introduction

The angle γ is defined as $\gamma = \arg[-V_{ud}V_{ub}^*/(V_{cd}V_{cb}^*)]$, where V_{ij} are the elements of the Cabibbo-Kobayashi-Maskawa (CKM) matrix [1]. It is one of the angles of the unitarity triangle and is to date the least well known angle of this triangle. At the same time it is the only angle that can be measured entirely with decays that only involve tree diagrams, so its measurement is largely unaffected by the theoretical uncertainty, which is $\mathcal{O}(10^{-6})$ [2]. Both Belle and BaBar have recently published averages of their measurements, each following a frequentist treatment. Belle measures $\gamma = (68_{-14}^{+15})^\circ$ [3], and BaBar measures $\gamma = (69_{-16}^{+17})^\circ$ [4]. In this work a combination of LHCb measurements is presented. World averages have been computed by the CKMfitter and UTfit groups, who obtain $\gamma = (66 \pm 12)^\circ$ [5], and $\gamma = (70.8 \pm 7.8)^\circ$ [6], using a frequentist and Bayesian treatment, respectively. These averages are dominated by measurements performed at the B factories, and part of all LHCb measurements combined in this work are already included.

When measuring γ in tree decays, an important channel is the $B^\pm \rightarrow DK^\pm$ mode, where the symbol D denotes an admixture of D^0 and \bar{D}^0 mesons. The D meson is reconstructed in a final state accessible to both flavour states, thus exploiting interference between the $b \rightarrow u\bar{c}s$ and $b \rightarrow \bar{c}us$ amplitudes. Throughout this Letter, charge conjugation applies, unless stated otherwise. The measurements are categorised by the D meson final state: CP eigenstates (GLW [7, 8]), quasi-flavour-specific states (ADS [9, 10]), and self-conjugate three-body final states (GGSZ [11]). The small theoretical uncertainty in the measurement of γ is obtained in these decays because all hadronic parameters are determined from data. The amplitude ratio $r_B^K = |A(B^- \rightarrow \bar{D}^0 K^-)/A(B^- \rightarrow D^0 K^-)|$, plays a crucial role as the uncertainty on γ scales roughly as $1/r_B^K$. It is measured to be $r_B^K \approx 0.1$ [3, 4].

Besides the $B^\pm \rightarrow DK^\pm$ channel, the $B^\pm \rightarrow D\pi^\pm$ decay also exhibits some sensitivity to γ . The theoretical framework is fully analogous to the $B^\pm \rightarrow DK^\pm$ case. However, the respective amplitude ratio r_B^π is expected to be an order of magnitude smaller than r_B^K , limiting the sensitivity. In this Letter, information from $B^\pm \rightarrow D\pi^\pm$ decays is included in the combined measurement of γ for the first time. The hadronic parameters describing the D decays are determined from data. To better constrain these parameters, measurements by CLEO are included [12], that themselves contain inputs from the Heavy Flavour Averaging Group (HFAG).

It has been shown that the determination of γ from $B^\pm \rightarrow Dh^\pm$ decays, where $h = \pi, K$, is affected by $D^0-\bar{D}^0$ mixing [10, 13–16]. It enters in two parts of the analysis: in the description of the B decays (*e.g.* through the amplitude $B^+ \rightarrow D^0 K^+ \rightarrow \bar{D}^0 K^+ \rightarrow f K^+$, where f denotes the D final state), and in the determination of the hadronic parameters that describe the D decay. Since D mixing is now well established, its effect is included in this combination; the CLEO measurement [12] also takes it into account explicitly. The effect of D mixing on the GLW, ADS, and GGSZ analyses is reviewed in Ref. [16]: it mostly affects the ADS analysis of $B^\pm \rightarrow D\pi^\pm$ decays, due to the small expected value of r_B^π . The ADS analysis of $B^\pm \rightarrow DK^\pm$ decays receives a shift of $|\Delta\gamma| \lesssim 1^\circ$ [16]. The Dalitz-model independent GGSZ analysis of $B^\pm \rightarrow DK^\pm$ is affected to a negligible extent [15, 16], and the GLW analyses of $B^\pm \rightarrow Dh^\pm$ are affected at most at order of $\mathcal{O}(r_B^K \sqrt{x_D^2 + y_D^2})$ [16],

where the mixing parameters x_D and y_D are at the level of 10^{-2} . Here, a D mixing measurement by LHCb [17] is included, to further constrain x_D and y_D .

The effect of possible CP violation in D decays to the $\pi^+\pi^-$ and K^+K^- final states [18, 19] has been discussed in Refs. [20–22]. This changes the interpretation of the observables of the GLW method, which is included as described in Sect. 2.2.

In this combination, the strategy is to maximise a total likelihood built from the product of the probability density functions (PDFs) f_i of experimental observables \vec{A}_i

$$\mathcal{L}(\vec{\alpha}) = \prod_i f_i(\vec{A}_i^{\text{obs}}|\vec{\alpha}), \quad (1)$$

where the \vec{A}_i^{obs} are the measured values of the observables, and $\vec{\alpha}$ is the set of parameters. The subscript i denotes the contributing inputs, summarised in Sects. 2.2–2.4. For most of the input measurements it is assumed that the observables follow a Gaussian distribution

$$f_i \propto \exp\left(-\frac{1}{2}(\vec{A}_i(\vec{\alpha}) - \vec{A}_i^{\text{obs}})^T V_i^{-1} (\vec{A}_i(\vec{\alpha}) - \vec{A}_i^{\text{obs}})\right), \quad (2)$$

where V_i is the experimental covariance matrix. In this combined measurement the statistical uncertainties dominate the resulting confidence intervals. Therefore it is assumed that the systematic fluctuations are also Gaussian, so that $V_i = V_i^{\text{stat}} + V_i^{\text{syst}}$. Since not all off-diagonal entries of V_i^{syst} have been published, they are assumed to be zero in the nominal result. An overall systematic uncertainty is estimated due to this assumption. Any other correlations across the statistically independent input measurements are neglected. For one pair of variables ($\kappa_{K3\pi}$, $\delta_{K3\pi}$, described in Sect. 2) that shows highly non-Gaussian behaviour, the experimental likelihood is taken into account. Table 1 defines all free parameters in the global fit. The amplitude ratios are defined as those of the suppressed processes divided by the favoured ones. Confidence intervals on γ and the most important hadronic parameters are set using a frequentist procedure. The statistical coverage of this procedure is evaluated.

2 Input measurements

The LHCb collaboration has published three analyses relevant to this paper based on the data corresponding to an integrated luminosity of 1.0 fb^{-1} using pp collisions at a centre-of-mass energy of 7 TeV, recorded in 2011. They are a GGSZ measurement of $B^\pm \rightarrow DK^\pm$ decays, where the D meson is reconstructed in the $D \rightarrow K_s^0 \pi^+ \pi^-$ and $D \rightarrow K_s^0 K^+ K^-$ final states [23]; a GLW/ADS measurement of $B^\pm \rightarrow DK^\pm$ and $B^\pm \rightarrow D\pi^\pm$ decays, where the D meson is reconstructed in charged two-body final states [24]; and an ADS measurement of $B^\pm \rightarrow DK^\pm$ and $B^\pm \rightarrow D\pi^\pm$ decays, where the D meson is reconstructed in charged four-body final states [25]. In addition, inputs from a combination of experimental data performed by the HFAG, to constrain the effect of direct CP violation in D decays [26], and measurements from the LHCb collaboration [17] and the CLEO collaboration [12], to constrain the hadronic parameters of the D system, are included. Ref. [12] includes itself inputs by the HFAG.

Table 1: Free parameters used in the combined fit. The phase differences $\delta_{K\pi}$ and $\delta_{K3\pi}$ are defined in accordance with Refs. [3, 4, 12], they are shifted by 180° with respect to the HFAG. Also, γ gains a sign for the conjugated modes, $A(B^+ \rightarrow D^0 h^+)/A(B^+ \rightarrow \bar{D}^0 h^+) = r_B^h e^{i(\delta_B^h + \gamma)}$, with $h = K, \pi$.

Decay	Description	Parameter
$B^\pm \rightarrow Dh^\pm$	CP -violating weak phase	γ
	$\Gamma(B^- \rightarrow D^0 K^-)/\Gamma(B^- \rightarrow D^0 \pi^-)$	R_{cab}
$B^\pm \rightarrow D\pi^\pm$	$A(B^- \rightarrow \bar{D}^0 \pi^-)/A(B^- \rightarrow D^0 \pi^-) = r_B^\pi e^{i(\delta_B^\pi - \gamma)}$	r_B^π, δ_B^π
$B^\pm \rightarrow DK^\pm$	$A(B^- \rightarrow \bar{D}^0 K^-)/A(B^- \rightarrow D^0 K^-) = r_B^K e^{i(\delta_B^K - \gamma)}$	r_B^K, δ_B^K
$D^0 \rightarrow K^\pm \pi^\mp$	$A(D^0 \rightarrow \pi^- K^+)/A(D^0 \rightarrow K^- \pi^+) = r_{K\pi} e^{-i\delta_{K\pi}}$	$r_{K\pi}, \delta_{K\pi}$
	Cabibbo-favoured rate	$\Gamma(D \rightarrow K\pi)$
$D^0 \rightarrow K^\pm \pi^\mp \pi^+ \pi^-$	amplitude ratio and effective strong phase diff.	$r_{K3\pi}, \delta_{K3\pi}$
	coherence factor	$\kappa_{K3\pi}$
	Cabibbo-favoured rate	$\Gamma(D \rightarrow K\pi\pi\pi)$
$D^0 \rightarrow K^+ K^-$	direct CP asymmetry	$A_{CP}^{\text{dir}}(KK)$
$D^0 \rightarrow \pi^+ \pi^-$	direct CP asymmetry	$A_{CP}^{\text{dir}}(\pi\pi)$
$D^0 - \bar{D}^0$	mixing parameters	x_D, y_D

2.1 Measurements from $B^\pm \rightarrow D[\rightarrow K_s^0 h^+ h^-]K^\pm$ decays

The GGSZ method [11] proposes the use of self-conjugate three-body D decays in the measurement of γ from $B^\pm \rightarrow DK^\pm$ processes. The variables x_\pm and y_\pm , defined as

$$x_\pm = r_B^K \cos(\delta_B^K \pm \gamma), \quad (3)$$

$$y_\pm = r_B^K \sin(\delta_B^K \pm \gamma), \quad (4)$$

are obtained from a fit to the Dalitz plane of $D \rightarrow K_s^0 \pi^+ \pi^-$ and $D \rightarrow K_s^0 K^+ K^-$ decays, separately for B^+ and B^- decays. The measurement, performed by LHCb, is reported in Ref. [23]. The study makes no model-dependent assumption on the variation of the strong phase of the $D \rightarrow K_s^0 h^+ h^-$ amplitudes, but instead uses measurements of this quantity from CLEO [27], as input. The reported results are

$$x_- = (0.0 \pm 4.3 \pm 1.5 \pm 0.6) \times 10^{-2}, \quad (5)$$

$$y_- = (2.7 \pm 5.2 \pm 0.8 \pm 2.3) \times 10^{-2}, \quad (6)$$

$$x_+ = (-10.3 \pm 4.5 \pm 1.8 \pm 1.4) \times 10^{-2}, \quad (7)$$

$$y_+ = (-0.9 \pm 3.7 \pm 0.8 \pm 3.0) \times 10^{-2}, \quad (8)$$

where the first uncertainty is statistical, the second is systematic, and the third is due to the external CLEO measurement. The non-vanishing statistical correlations are $\rho(x_-, y_-) = -0.11$, $\rho(x_+, y_+) = +0.17$, and the relevant systematic correlations are $\rho(x_-, y_-) = -0.05$, and $\rho(x_+, y_+) = +0.36$.

The GGSZ method can also be applied to $B^\pm \rightarrow D\pi^\pm$ final states. In Ref. [23] this was not performed, since these final states were needed to control the efficiency variation across the Dalitz plot. The effect of $D^0\text{--}\bar{D}^0$ mixing in the measurement of the x_\pm and y_\pm in Eqns. 5–8 is suppressed, leading to a negligible effect in the extraction of γ [15, 16].

2.2 Measurements from $B^\pm \rightarrow D[\rightarrow h^+h^-]h^\pm$ decays

The D decay modes considered in the analysis of two-body D final states [24] are $D \rightarrow K^+K^-$, $D \rightarrow \pi^+\pi^-$, the favoured decay $D \rightarrow K^-\pi^+$, where the kaon charge matches that of the h^\pm track from the $B^\pm \rightarrow Dh^\pm$ decay (called $K\pi$ in the following), and the suppressed decay $D \rightarrow \pi^-K^+$, where the kaon charge is opposite that of the h^\pm track (called πK in the following). Building on the initial GLW/ADS ideas [7–10], a set of 13 observables was defined by forming ratios of decay rates, defined below, such that many systematic uncertainties cancel. The charge-averaged ratios of $B^\pm \rightarrow DK^\pm$ and $B^\pm \rightarrow D\pi^\pm$ decays are

$$R_{K/\pi}^f = \frac{\Gamma(B^- \rightarrow D[\rightarrow f]K^-) + \Gamma(B^+ \rightarrow D[\rightarrow \bar{f}]K^+)}{\Gamma(B^- \rightarrow D[\rightarrow f]\pi^-) + \Gamma(B^+ \rightarrow D[\rightarrow \bar{f}]\pi^+)} , \quad (9)$$

where f is the relevant final state. The ratios $R_{K/\pi}^f$ are related to γ and the hadronic parameters through

$$R_{K/\pi}^f = R_{\text{cab}} \frac{1 + (r_B^K r_f)^2 + 2r_B^K r_f \kappa \cos(\delta_B^K - \delta_f) \cos \gamma + M_-^K + M_+^K}{1 + (r_B^\pi r_f)^2 + 2r_B^\pi r_f \kappa \cos(\delta_B^\pi - \delta_f) \cos \gamma + M_-^\pi + M_+^\pi} , \quad (10)$$

for the favoured final state $f = K\pi$, where the coherence factor κ in Eq. 10 (and in all following equations in this Section) is unity for two-body decays, and through

$$R_{K/\pi}^f = R_{\text{cab}} \frac{1 + (r_B^K)^2 + 2r_B^K \cos \delta_B^K \cos \gamma}{1 + (r_B^\pi)^2 + 2r_B^\pi \cos \delta_B^\pi \cos \gamma} , \quad (11)$$

for $f = KK, \pi\pi$. The D mixing correction terms M_\pm^h are, at leading order in x_D and y_D , and neglecting CP violation in D mixing, given by [13]

$$M_\pm^h = (\kappa r_f ((r_B^h)^2 - 1) \sin \delta_f + r_B^h (1 - r_f^2) \sin(\delta_B^h \pm \gamma)) a_D x_D \\ - (\kappa r_f ((r_B^h)^2 + 1) \cos \delta_f + r_B^h (1 + r_f^2) \cos(\delta_B^h \pm \gamma)) a_D y_D . \quad (12)$$

The D mixing corrections depend on the D decay time acceptance and resolution in the reconstruction of $B^\pm \rightarrow Dh^\pm$ decays [16]. The coefficient a_D parameterises their effect. It takes the value of $a_D = 1$ in case of an ideal, flat acceptance and negligible time resolution. For a realistic acceptance and resolution model present in the GLW/ADS analysis of Ref. [24], it is estimated to be $a_D = 1.20 \pm 0.04$, where the uncertainty can be safely neglected in this combination. For CP even final states of the D meson, the mixing

corrections cancel exactly in Eq. 11 (and 15), as in this case $\kappa = 1$, $r_f = 1$, $\delta_f = 0$. The charge asymmetries are

$$A_h^f = \frac{\Gamma(B^- \rightarrow D[\rightarrow f]h^-) - \Gamma(B^+ \rightarrow D[\rightarrow \bar{f}]h^+)}{\Gamma(B^- \rightarrow D[\rightarrow f]h^-) + \Gamma(B^+ \rightarrow D[\rightarrow \bar{f}]h^+)}, \quad (13)$$

which are related to γ and the hadronic parameters through

$$A_h^f = \frac{2r_B^h r_f \kappa \sin(\delta_B^h - \delta_f) \sin \gamma + M_-^h - M_+^h}{1 + (r_B^h r_f)^2 + 2r_B^h r_f \kappa \cos(\delta_B^h - \delta_f) \cos \gamma + M_-^h + M_+^h}, \quad (14)$$

for the favoured final state $f = K\pi$, and through

$$A_h^f = \frac{2r_B^h \sin \delta_B^h \sin \gamma}{1 + (r_B^h)^2 + 2r_B^h \cos \delta_B^h \cos \gamma}, \quad (15)$$

for $f = KK, \pi\pi$, where r_B^h denotes r_B^K and r_B^π . Finally, the non charge-averaged ratios of suppressed and favoured D final states are

$$\begin{aligned} R_h^\pm &= \frac{\Gamma(B^\pm \rightarrow D[\rightarrow f_{\text{sup}}]h^\pm)}{\Gamma(B^\pm \rightarrow D[\rightarrow f]h^\pm)} \\ &= \frac{r_f^2 + (r_B^h)^2 + 2r_B^h r_f \kappa \cos(\delta_B^h + \delta_f \pm \gamma) - [M_\pm^h]_{\text{sup}}}{1 + (r_B^h r_f)^2 + 2r_B^h r_f \kappa \cos(\delta_B^h - \delta_f \pm \gamma) + M_\pm^h}, \end{aligned} \quad (16)$$

where $f_{\text{sup}} = \pi K$ is the suppressed final state, and $f = K\pi$ the allowed one. The suppressed D mixing correction terms are given, at leading order in x_D and y_D , by

$$\begin{aligned} [M_\pm^h]_{\text{sup}} &= (\kappa r_f ((r_B^h)^2 - 1) \sin \delta_f + r_B^h (1 - r_f^2) \sin(\delta_B^h \pm \gamma)) a_D x_D \\ &\quad + (\kappa r_f ((r_B^h)^2 + 1) \cos \delta_f + r_B^h (1 + r_f^2) \cos(\delta_B^h \pm \gamma)) a_D y_D. \end{aligned} \quad (17)$$

The combination makes use of all γ -sensitive observables determined in the GLW/ADS analysis. The full set, taken from the two-body analysis [24], is

$$\begin{aligned} R_{K/\pi}^{K\pi} &= 0.0774 \pm 0.0012 \pm 0.0018, \\ R_{K/\pi}^{KK} &= 0.0773 \pm 0.0030 \pm 0.0018, \\ R_{K/\pi}^{\pi\pi} &= 0.0803 \pm 0.0056 \pm 0.0017, \\ A_\pi^{K\pi} &= -0.0001 \pm 0.0036 \pm 0.0095, \\ A_K^{K\pi} &= 0.0044 \pm 0.0144 \pm 0.0174, \\ A_K^{KK} &= 0.148 \pm 0.037 \pm 0.010, \\ A_K^{\pi\pi} &= 0.135 \pm 0.066 \pm 0.010, \\ A_\pi^{KK} &= -0.020 \pm 0.009 \pm 0.012, \\ A_\pi^{\pi\pi} &= -0.001 \pm 0.017 \pm 0.010, \\ R_K^- &= 0.0073 \pm 0.0023 \pm 0.0004, \\ R_K^+ &= 0.0232 \pm 0.0034 \pm 0.0007, \\ R_\pi^- &= 0.00469 \pm 0.00038 \pm 0.00008, \\ R_\pi^+ &= 0.00352 \pm 0.00033 \pm 0.00007, \end{aligned}$$

where the first uncertainty is statistical and the second systematic. Their statistical correlations, not previously published, are given in Table 2.

Direct CP asymmetries in $D^0 \rightarrow K^+K^-$ and $D^0 \rightarrow \pi^+\pi^-$ decays have been measured [18, 19]. While the effect on the charge averaged ratios $R_{K/\pi}^{KK}$ and $R_{K/\pi}^{\pi\pi}$ is negligible [21], the observables A_h^{KK} and $A_h^{\pi\pi}$ are modified by adding the respective direct CP asymmetry A_{CP}^{dir} to the right-hand side of Eq. 15. This is valid up to neglecting a small weak phase in the D decay [21]. The HFAG results on A_{CP}^{dir} [26] are included in this combination

$$A_{CP}^{\text{dir}}(KK) = (-0.31 \pm 0.24) \times 10^{-2},$$

$$A_{CP}^{\text{dir}}(\pi\pi) = (+0.36 \pm 0.25) \times 10^{-2}.$$

These quantities are correlated, $\rho(A_{CP}^{\text{dir}}(KK), A_{CP}^{\text{dir}}(\pi\pi)) = +0.80$, and therefore they are constrained to their observed values by means of a two-dimensional correlated Gaussian PDF. The inclusion of the result on $A_{CP}^{\text{dir}}(KK) - A_{CP}^{\text{dir}}(\pi\pi)$ [18], which is statistically independent from the HFAG average, is found to have no effect on the combination.

2.3 Measurements from $B^\pm \rightarrow D[\rightarrow K^\pm\pi^\mp\pi^+\pi^-]h^\pm$ decays

The D four-body decay modes considered in the analysis of Ref. [25] are the favoured $D \rightarrow K^-\pi^+\pi^-\pi^+$, and the suppressed $D \rightarrow \pi^-K^+\pi^-\pi^+$ final states. In a similar manner to the two-body GLW/ADS analysis, seven observables are defined as ratios of decay rates. Their relations to γ and the hadronic parameters are fully analogous and given by Eqs. 10, 14, and 16, with $f = K\pi\pi\pi$ and $f_{\text{sup}} = \pi K\pi\pi$. The CP -violating effects are diluted due to the D decay proceeding through a range of resonances that can only interfere in limited regions of the four-body phase space. This dilution is accounted for by multiplying each interference term by a coherence factor $\kappa = \kappa_{K3\pi}$. The D decay time

Table 2: Statistical correlations of the $B^\pm \rightarrow Dh^\pm$, $D \rightarrow hh$ analysis [24].

	A_K^{KK}	A_π^{KK}	$A_K^{\pi\pi}$	$A_\pi^{\pi\pi}$	$A_K^{K\pi}$	$A_\pi^{K\pi}$	$R_{K/\pi}^{\pi\pi}$	$R_{K/\pi}^{KK}$	$R_{K/\pi}^{K\pi}$	R_K^-	R_π^-	R_K^+	R_π^+
A_K^{KK}	1	-0.029	0	0	0	0	-0.002	-0.034	-0.010	-0.001	0	0	0
A_π^{KK}		1	0	0	0	0	0	-0.003	0	0	0	0	0
$A_K^{\pi\pi}$			1	-0.032	0	0	-0.032	-0.002	-0.004	-0.001	0	0	0
$A_\pi^{\pi\pi}$				1	0	0	-0.004	0	0	0	0	0	0
$A_K^{K\pi}$					1	-0.045	0	0	0.003	0.004	0	-0.004	-0.001
$A_\pi^{K\pi}$						1	0	0	-0.001	0.004	0.002	-0.004	-0.002
$R_{K/\pi}^{\pi\pi}$							1	0.013	0.029	0.003	0.003	0.001	0.003
$R_{K/\pi}^{KK}$								1	0.053	0.005	0.005	0.002	0.004
$R_{K/\pi}^{K\pi}$									1	-0.038	0.016	-0.093	0.014
R_K^-										1	-0.023	0.012	0.006
R_π^-											1	0.005	0.008
R_K^+												1	-0.036
R_π^+													1

acceptance and resolution model is identical to that present in the two-body GLW/ADS analysis of Ref. [24]. The seven observables, taken from the four-body analysis reported in Ref. [25], are

$$\begin{aligned}
R_{K/\pi}^{K3\pi} &= 0.0765 \pm 0.0017 \pm 0.0026, \\
A_{\pi}^{K3\pi} &= -0.006 \pm 0.005 \pm 0.010, \\
A_K^{K3\pi} &= -0.026 \pm 0.020 \pm 0.018, \\
R_{K^-}^{K3\pi} &= 0.0071 \pm 0.0034 \pm 0.0008, \\
R_{K^+}^{K3\pi} &= 0.0155 \pm 0.0042 \pm 0.0010, \\
R_{\pi^-}^{K3\pi} &= 0.00400 \pm 0.00052 \pm 0.00011, \\
R_{\pi^+}^{K3\pi} &= 0.00316 \pm 0.00046 \pm 0.00011,
\end{aligned}$$

where the first uncertainty is statistical and the second systematic. The statistical correlations between these variables, not previously published, are presented in Table 3.

Table 3: Statistical correlations of the $B^{\pm} \rightarrow Dh^{\pm}$, $D \rightarrow K\pi\pi\pi$ analysis [25].

	$R_{K/\pi}^{K3\pi}$	$A_K^{K3\pi}$	$A_{\pi}^{K3\pi}$	$R_{K^-}^{K3\pi}$	$R_{K^+}^{K3\pi}$	$R_{\pi^-}^{K3\pi}$	$R_{\pi^+}^{K3\pi}$
$R_{K/\pi}^{K3\pi}$	1	0.003	0.001	-0.060	-0.024	0.017	0.021
$A_K^{K3\pi}$		1	-0.035	-0.007	0.006	-0.002	0.002
$A_{\pi}^{K3\pi}$			1	-0.006	0.008	-0.002	0.005
$R_{K^-}^{K3\pi}$				1	0.043	0.006	0.029
$R_{K^+}^{K3\pi}$					1	0.022	0.025
$R_{\pi^-}^{K3\pi}$						1	0.032
$R_{\pi^+}^{K3\pi}$							1

2.4 Measurement of the hadronic parameters of the D system from $D^0 \rightarrow K^{\pm}\pi^{\mp}$, $K^{\pm}\pi^{\mp}\pi^+\pi^-$ decays by CLEO

The two- and four-body ADS measurements both reach their best sensitivity when combined with knowledge of the hadronic parameters of the D decay. These are, for the $D^0 \rightarrow K^{\pm}\pi^{\mp}$ decays, the amplitude ratio $r_{K\pi}$ and the strong phase difference $\delta_{K\pi}$. The hadronic parameters of the $D^0 \rightarrow K^{\pm}\pi^{\mp}\pi^+\pi^-$ decays are the ratio $r_{K3\pi}$, the phase $\delta_{K3\pi}$ and the coherence factor¹ $\kappa_{K3\pi}$. All of these parameters are constrained by a CLEO measurement [12], where a combined fit is performed, which includes information on the D mixing parameters and the Cabibbo-favoured branching fractions of the D decay through the following relationship

$$\frac{\Gamma(D^0 \rightarrow f_{\text{sup}})}{\Gamma(D^0 \rightarrow f_{\text{fav}})} = r_f^2 \left[1 - \frac{y_D}{r_f} \kappa \cos \delta_f + \frac{x_D}{r_f} \kappa \sin \delta_f + \frac{x_D^2 + y_D^2}{2r_f^2} \right], \quad (18)$$

¹Note that Ref. [12] uses the symbol $R_{K3\pi}$ to denote the coherence factor.

where $r_f = r_{K\pi}$ ($r_{K3\pi}$), $\delta_f = \delta_{K\pi}$ ($\delta_{K3\pi}$), and $\kappa = 1$ ($\kappa_{K3\pi}$), for $D^0 \rightarrow K^\pm \pi^\mp$ ($K^\pm \pi^\mp \pi^+ \pi^-$) decays. All of these parameters are included in the combination, although the dependence of γ on the D mixing parameters and the Cabibbo-favoured branching fractions is small compared to the current statistical precision. The central values and the uncertainties given in Table 4 are reproduced from the analysis by the CLEO collaboration reported in Ref. [12]. The covariance matrix (see Table VI in Ref. [12]) is also used, though it is not reproduced here. The parameters ($\delta_{K3\pi}, \kappa_{K3\pi}$) exhibit a non-Gaussian two-dimensional likelihood (see Fig. 2b in Ref. [12]), and this likelihood is used in the combination [28]. Their central values and profile-likelihood uncertainties are $\kappa_{K3\pi} = 0.33^{+0.26}_{-0.23}$ and $\delta_{K3\pi} = (114^{+26}_{-23})^\circ$. Correlations of $\delta_{K3\pi}$ and $\kappa_{K3\pi}$ to other parameters are neglected.

Table 4: Results of the CLEO measurement [12].

Observable	Central value and uncertainty
$\delta_{K\pi}$	$(-151.5^{+9.6}_{-9.5})^\circ$
x_D	$(0.96 \pm 0.25) \times 10^{-2}$
y_D	$(0.81 \pm 0.16) \times 10^{-2}$
$\mathcal{B}(D^0 \rightarrow K^- \pi^+)$	$(3.89 \pm 0.05) \times 10^{-2}$
$\mathcal{B}(D^0 \rightarrow \pi^- K^+)$	$(1.47 \pm 0.07) \times 10^{-4}$
$\mathcal{B}(D^0 \rightarrow K^- \pi^+ \pi^- \pi^+)$	$(7.96 \pm 0.19) \times 10^{-2}$
$\mathcal{B}(D^0 \rightarrow \pi^- K^+ \pi^- \pi^+)$	$(2.65 \pm 0.19) \times 10^{-4}$

2.5 Measurement from $D^0 \rightarrow K^\pm \pi^\mp$ decays by LHCb

The D mixing parameters x_D and y_D are constrained in addition by an LHCb measurement of $D^0 \rightarrow K^\pm \pi^\mp$ decays [17]. Three observables are defined, R_D , y'_D , and $x_D'^2$, that are related to the D system parameters through the following relationships

$$R_D = r_{K\pi}^2, \quad (19)$$

$$y'_D = x_D \sin \delta_{K\pi} - y_D \cos \delta_{K\pi}, \quad (20)$$

$$x_D'^2 = (x_D \cos \delta_{K\pi} + y_D \sin \delta_{K\pi})^2, \quad (21)$$

where a phase shift of 180° was introduced to $\delta_{K\pi}$ to be in accordance with the phase convention adopted in this Letter. In Ref. [17], the measured central values of the observables are $R_D = (3.52 \pm 0.15) \times 10^{-3}$, $y'_D = (7.2 \pm 2.4) \times 10^{-3}$, and $x_D'^2 = (-0.09 \pm 0.13) \times 10^{-3}$, where the error includes both statistical and systematic uncertainties. These observables are strongly correlated, $\rho(R_D, y'_D) = -0.95$, $\rho(y'_D, x_D'^2) = -0.97$, and $\rho(x_D'^2, R_D) = +0.88$. They are included by means of a three-dimensional correlated Gaussian PDF.

3 Statistical interpretation

The evaluation of this combination follows a frequentist approach. A χ^2 -function is defined as $\chi^2(\vec{\alpha}) = -2 \ln \mathcal{L}(\vec{\alpha})$, where $\mathcal{L}(\vec{\alpha})$ is defined in Eq. 1. The best-fit point is given by the global minimum of the χ^2 -function, $\chi^2(\vec{\alpha}_{\min})$. To evaluate the confidence level for a given value of a certain parameter, say $\gamma = \gamma_0$ in the following, the value of the χ^2 -function at the new minimum is considered, $\chi^2(\vec{\alpha}'_{\min}(\gamma_0))$. This also defines the profile likelihood function $\hat{\mathcal{L}}(\gamma_0) = \exp(-\chi^2(\vec{\alpha}'_{\min}(\gamma_0))/2)$. Then a test statistic is defined as $\Delta\chi^2 = \chi^2(\vec{\alpha}'_{\min}(\gamma_0)) - \chi^2(\vec{\alpha}_{\min})$. The p -value, or $1 - \text{CL}$, is calculated by means of a Monte Carlo procedure, described in Ref. [29] and briefly recapitulated here. For each value of γ_0 :

1. $\Delta\chi^2$ is calculated;
2. a set of pseudoexperiments \vec{A}_j is generated using Eq. 1 with parameters $\vec{\alpha}$ set to $\vec{\alpha}'_{\min}$ as the PDF;
3. $\Delta\chi^{2'}$ of the pseudoexperiment is calculated by replacing $\vec{A}_{\text{obs}} \rightarrow \vec{A}_j$ and minimising with respect to $\vec{\alpha}$, once with γ as a free parameter, and once with γ fixed to γ_0 ;
4. $1 - \text{CL}$ is calculated as the fraction of pseudoexperiments which perform worse ($\Delta\chi^2 < \Delta\chi^{2'}$) than the measured data.

This method is sometimes known as the “ $\hat{\mu}$ ”, or the “plug-in” method. Its coverage cannot be guaranteed [29] for the full parameter space, but is verified for the best-fit point. The reason is, that at each point γ_0 , the nuisance parameters, *i.e.* the components of $\vec{\alpha}$ other than the parameter of interest, are set to their best-fit values for this point, as opposed to computing an n -dimensional confidence belt, which is computationally very demanding.

In case of the CLEO likelihood for $\kappa_{K3\pi}$ and $\delta_{K3\pi}$, it is assumed that the true PDF, for any assumed true value of $\kappa_{K3\pi}$ and $\delta_{K3\pi}$, can be described by a shifted version of the likelihood profile. In the non-physical range, $\kappa_{K3\pi} \notin [0, 1]$, the likelihood profile is not available. It is extrapolated into the non-physical range using Gaussian tails that correspond to the published uncertainties of the central value. If $H(x, y)$ denotes the provided likelihood profile, with a maximum at position (\hat{x}, \hat{y}) , it is transformed as $f_i(x_{\text{obs}}, y_{\text{obs}} | x, y) \propto H_i(x - x_{\text{obs}} + \hat{x}, y - y_{\text{obs}} + \hat{y})$, with the abbreviation $(x, y) = (\kappa_{K3\pi}, \delta_{K3\pi})$.

4 Results

Three different combinations are presented. First, only the parts corresponding to $B^\pm \rightarrow DK^\pm$ decays of the two- and four-body GLW/ADS measurements [24, 25] are combined with the GGSZ [23] measurement. Then, only the $B^\pm \rightarrow D\pi^\pm$ parts of the two- and four-body GLW/ADS measurements are combined. Finally, the full $B^\pm \rightarrow Dh^\pm$ combination is computed. It is difficult to disentangle the $B^\pm \rightarrow DK^\pm$ and $B^\pm \rightarrow D\pi^\pm$ measurements, because the observed ratios of Eq. 9 necessarily contain information on both systems. These

ratios are therefore included in the $B^\pm \rightarrow DK^\pm$ combination, but not in the $B^\pm \rightarrow D\pi^\pm$ combination. To include them in the $B^\pm \rightarrow DK^\pm$ combination, the denominator in the second term of Eq. 10 is assumed to equal unity, neglecting a correction smaller than 0.04, such that effects of hadronic parameters in the $B^\pm \rightarrow D\pi^\pm$ system are avoided. The separate DK^\pm ($D\pi^\pm$) combination contains 29 (22) observables, and the full combination contains 38 observables, as 13 observables from CLEO, HFAG, and Ref. [17] are common to both separate combinations. The results are summarised in Tables 5–7, and illustrated in Figs. 1–3. The equations of Sect. 2 are invariant under the simultaneous transformation $\gamma \rightarrow \gamma + 180^\circ$, $\delta \rightarrow \delta + 180^\circ$, where $\delta = \delta_B^K, \delta_B^\pi$. All results on γ , δ_B^K , and δ_B^π are expressed modulo 180° , and only the solution most consistent with the average computed by CKMfitter and UTfit is shown. Figure 4 shows two-dimensional profile likelihood contours of the full combination, where the discrete symmetry is apparent in subfigures (b) and (d). The DK^\pm combination results in confidence intervals for γ that are symmetric and almost Gaussian up to 95% CL. Beyond that a secondary, local minimum of $\chi^2(\alpha'_{\min})$ causes a much enlarged interval at 99% CL. The $D\pi^\pm$ combination results in unexpectedly small confidence intervals at 68% CL. This can be explained by an upward fluctuation of r_B^π , since again the uncertainty of γ scales roughly like $1/r_B^\pi$. The ratio r_B^π is expected to be $r_B^\pi \approx |(V_{ub}^*V_{cd})/(V_{cb}^*V_{ud})| \times |C|/|T+C| \approx 0.006$, where C and T describe the magnitudes of the colour-suppressed and tree amplitudes governing $B^\pm \rightarrow D\pi^\pm$ decays, with their numerical values estimated from Ref. [30]. Within the 95% CL interval, r_B^π is well consistent with this expectation, and no constraints on γ are set. The high value of r_B^π also affects the full combination.

Table 5: Confidence intervals and best-fit values of the DK^\pm combination for γ , δ_B^K , and r_B^K .

Quantity	DK^\pm combination
γ	72.0°
68% CL	$[56.4, 86.7]^\circ$
95% CL	$[42.6, 99.6]^\circ$
δ_B^K	112°
68% CL	$[96, 126]^\circ$
95% CL	$[80, 136]^\circ$
r_B^K	0.089
68% CL	$[0.080, 0.098]$
95% CL	$[0.071, 0.107]$

Table 6: Confidence intervals and best-fit values for the $D\pi^\pm$ combination for γ , δ_B^π , and r_B^π . The corrections to the γ intervals for undercoverage and neglected systematic correlations, as described in Sect. 5, are not yet applied.

Quantity	$D\pi^\pm$ combination
γ	18.9°
68% CL	[8.9, 80.2]° \cup [169.1, 175.7]°
95% CL	no constraint
δ_B^π	261°
68% CL	[213, 229]° \cup [249, 331]°
95% CL	no constraint
r_B^π	0.015
68% CL	[0.006, 0.056]
95% CL	[0.001, 0.073]

Table 7: Confidence intervals and best-fit values for the DK^\pm and $D\pi^\pm$ combination for γ , r_B^K , δ_B^K , r_B^π , and δ_B^π . The corrections to the γ intervals for undercoverage and neglected systematic correlations, as described in Sect. 5, are not yet applied.

Quantity	DK^\pm and $D\pi^\pm$ combination
γ	72.6°
68% CL	[56.7, 81.7]°
95% CL	[41.2, 92.3]°
r_B^K	0.089
68% CL	[0.080, 0.097]
95% CL	[0.071, 0.105]
δ_B^K	112°
68% CL	[96, 125]°
95% CL	[79, 136]°
r_B^π	0.015
68% CL	[0.006, 0.027]
95% CL	[0.002, 0.036]
δ_B^π	315°
68% CL	[269, 332]
95% CL	no constraint

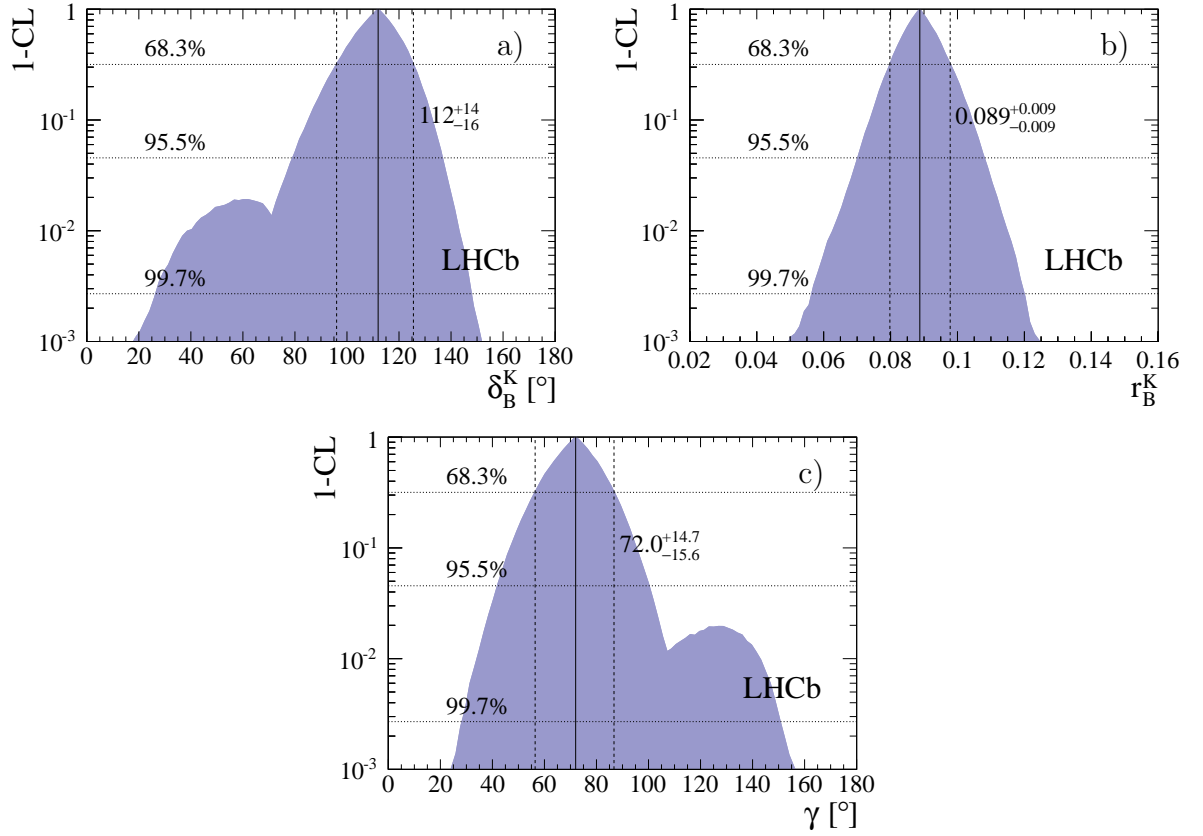


Figure 1: Graphs showing $1 - \text{CL}$ for (a) δ_B^K , (b) r_B^K , and (c) γ , for the DK^\pm combination of the two- and four-body GLW/ADS and the DK^\pm GGSZ measurements. The reported numbers correspond to the best-fit values and the uncertainties are computed using the respective 68.3% CL confidence interval shown in Table 5.

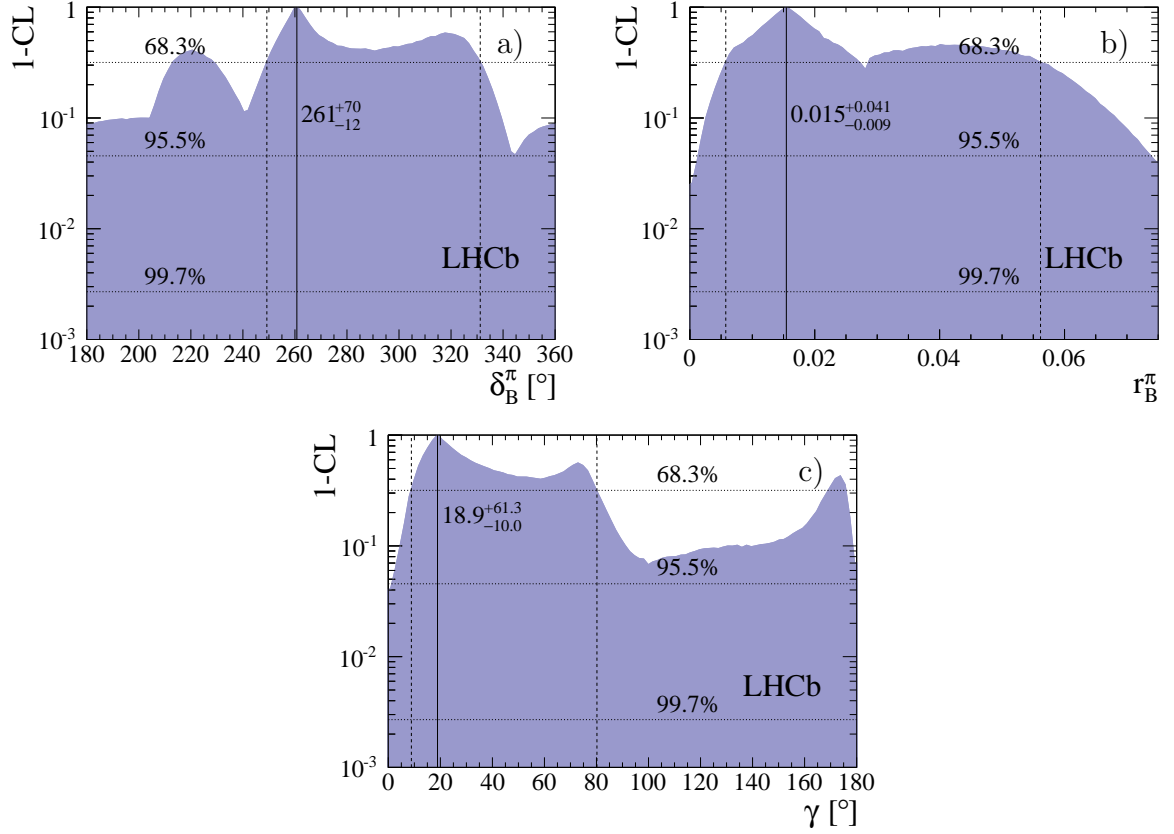


Figure 2: Graphs showing $1 - \text{CL}$ for (a) δ_B^π , (b) r_B^π , and (c) γ , for the $D\pi^\pm$ combination of the two- and four-body GLW/ADS measurements. The reported numbers correspond to the best-fit values and the uncertainties are computed using appropriate 68.3% CL confidence intervals shown in Table 6.

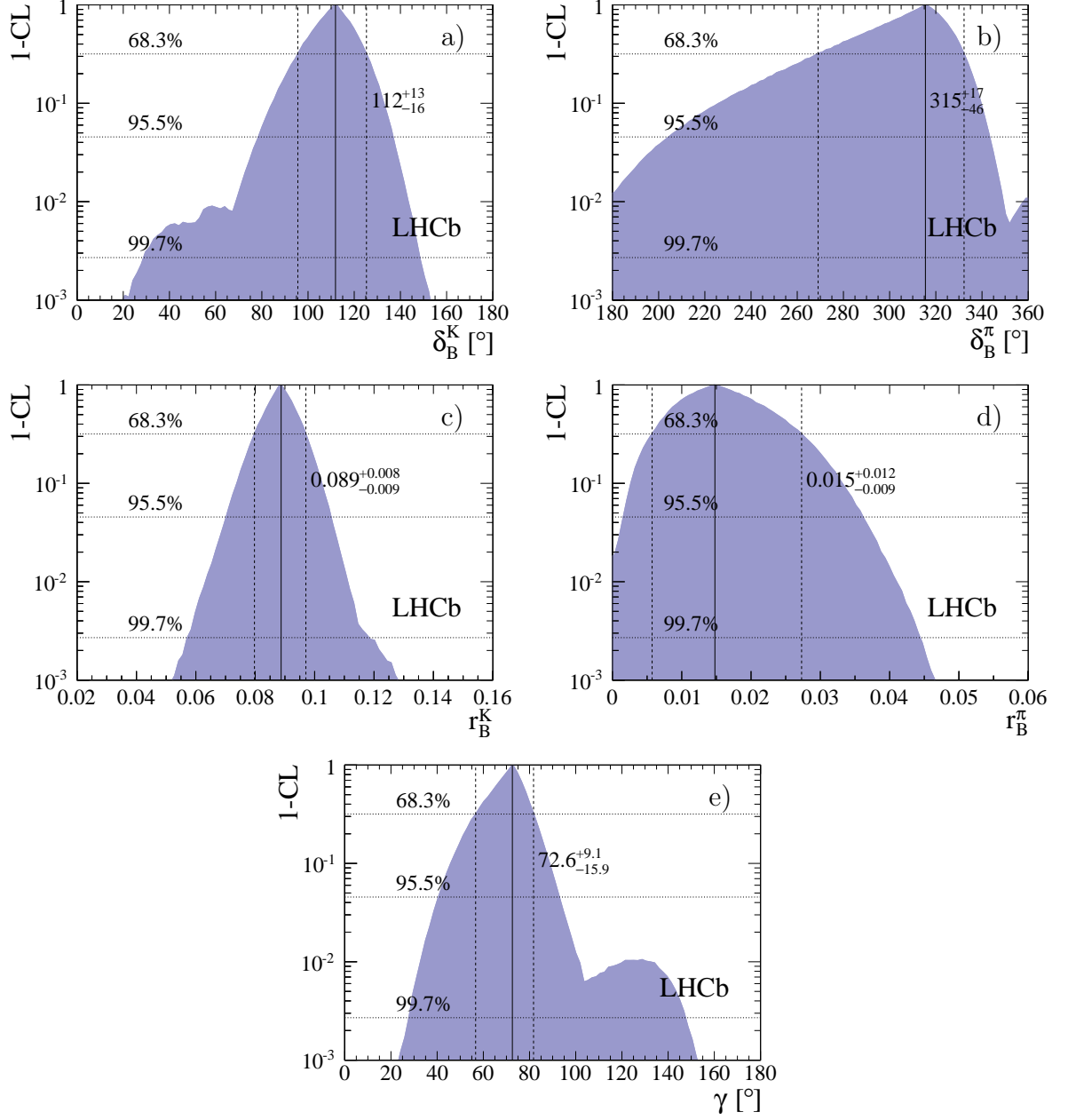


Figure 3: Graphs showing $1 - \text{CL}$ for (a) δ_B^K , (b) δ_B^π , (c) r_B^K , (d) r_B^π , and (e) γ , for the full DK^\pm and $D\pi^\pm$ combination. The reported numbers correspond to the best-fit values and the uncertainties are computed using appropriate 68.3% CL confidence intervals shown in Table 7.

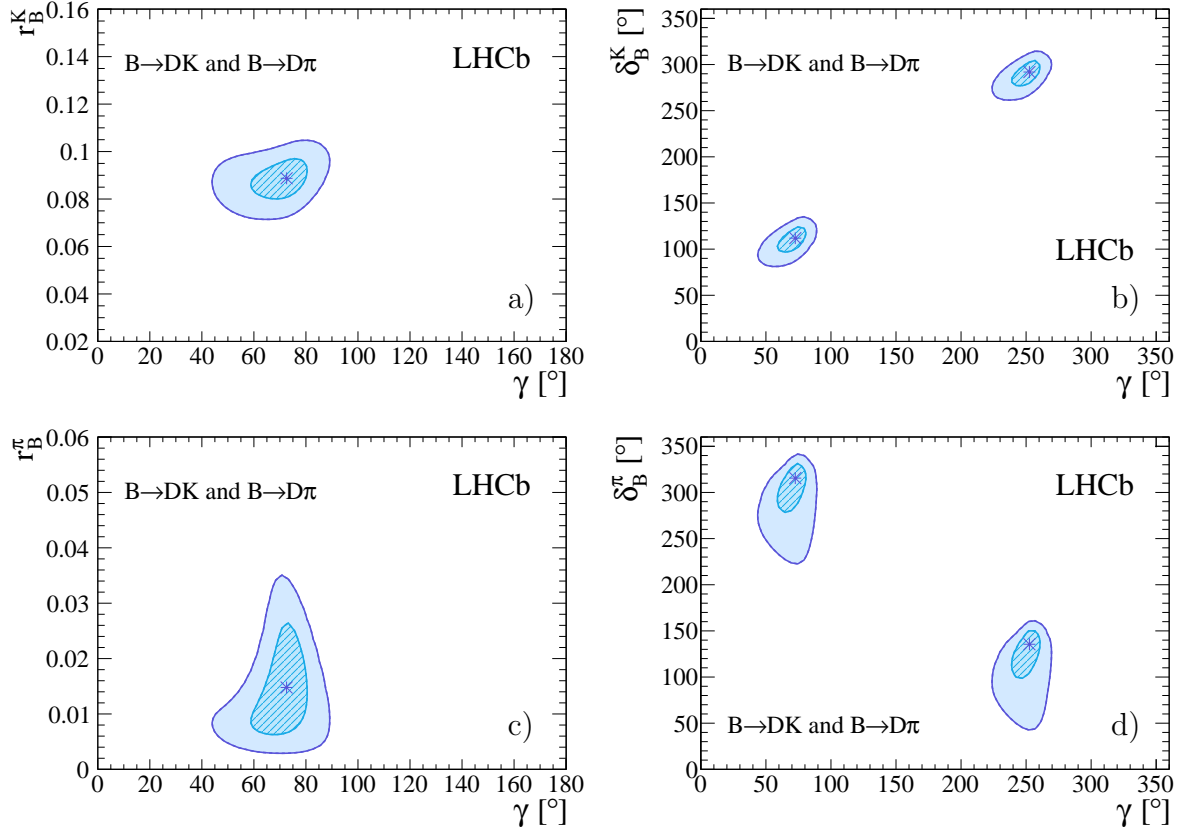


Figure 4: Profile likelihood contours of (a) γ vs. r_B^K , (b) γ vs. δ_B^K , (c) γ vs. r_B^π , and (d) γ vs. δ_B^π , for the full DK^\pm and $D\pi^\pm$ combination. The contours are the $n\sigma$ profile likelihood contours, where $\Delta\chi^2 = n^2$ with $n = 1, 2$. The markers denote the best-fit values. Subfigures (b) and (d) show the full angular range to visualize the symmetry, while subfigures (a) and (c) are expressed modulo 180° .

5 Validation of results and systematic uncertainties

To assess the agreement between the various input measurements, the probability P , that the observed dataset agrees better with the best-fit model than a dataset generated assuming that model, is considered. It is computed in two different ways. A first estimation of P is obtained as the p -value of a χ^2 test on the value $\chi^2(\vec{\alpha}_{\min})$, assuming it follows the χ^2 distribution with a number of degrees of freedom given by the difference of the the number of observables n_{obs} and the number of fit parameters n_{fit} . A more accurate approach is to generate pseudodatasets j at the best-fit value, and fit these datasets with all parameters free. Then P is given as the fraction of pseudoexperiments that satisfy ($\chi_j^2 > \chi_{\text{data}}^2$). For this test, the pseudoexperiments used for the plug-in method are re-evaluated. The fit probability based on the χ^2 distribution is well consistent with that based on the pseudoexperiments, as shown in Table 8.

The statistical coverage of the plug-in method is not guaranteed. Therefore the coverage is computed at the best-fit point for each of the three combinations. This is done by generating pseudodatasets at the best-fit point, and then, for each dataset, computing the p -value of the best-fit point using the plug-in method. The coverage is then defined as the fraction α in which the best-fit value of γ has a larger p -value than $\eta = 68.27\%$, $\eta = 95.45\%$, and $\eta = 99.73\%$, for 1-, 2-, 3σ , respectively. The plug-in method slightly undercovers in the $D\pi^\pm$ and full combinations, as shown in Table 9. The DK combination has exact coverage. The same table also contains the coverage of the simpler interval setting approach, in which the confidence intervals are defined by $\Delta\chi^2 = n^2$, where $n = 1, 2, 3$. The profile likelihood approach was found to significantly undercover. The DK^\pm combination has exact coverage. For the $D\pi^\pm$ and full combinations, the final plug-in confidence intervals (Tabs. 6, 7) are scaled up by factors η/α , taken from Table 9.

In addition the confidence intervals were cross-checked using a method inspired by Berger and Boos [31]. Instead of setting the nuisance parameters $\vec{\theta}$ to their best-fit values when computing the p -value, $p(\gamma_0, \vec{\theta})$, $n_{\text{BB}} = 50$ alternative points are chosen, drawn from an $(n_{\text{fit}} - 1)$ -dimensional uniform distribution over a restricted region C_β . Then, the p -value is given as $p_{\text{BB}} = \max_{\vec{\theta} \in C_\beta} p(\gamma_0, \vec{\theta}) + \beta$. Here, β is the probability that $\vec{\theta}$ lies outside C_β , and C_β is chosen large enough such that $\beta < 10^{-4}$. This method is more conservative than the nominal plug-in method, but is guaranteed to not undercover for $n_{\text{BB}} \rightarrow \infty$. The resulting intervals are only slightly larger than the nominal ones.

Table 8: Numbers of observables n_{obs} , numbers of free parameters in the fit n_{fit} , the minimum χ^2 at the best-fit point, and fit probabilities of the best-fit point for the three combinations. The quoted uncertainties are due to the limited number of pseudoexperiments.

Combination	n_{obs}	n_{fit}	χ_{\min}^2	$P[\%]$ (χ^2 distribution)	$P[\%]$ (pseudoexperiments)
DK^\pm	29	15	10.48	72.6	73.9 ± 0.2
$D\pi^\pm$	22	14	6.28	61.6	61.2 ± 0.3
full	38	17	13.06	90.6	90.9 ± 0.1

Table 9: Coverage fraction $f_{\text{in}} = N_{\text{in}}/N$ for γ at its best measured value for 1-, 2-, and 3σ intervals, for the plug-in method and the simpler approach based on the profile likelihood. The quoted uncertainties are due to the limited number of pseudoexperiments.

Combination	η	α (plug-in)	α (profile likelihood)
DK^\pm	0.6827 (1σ)	0.6874 ± 0.0050	0.6508 ± 0.0051
	0.9545 (2σ)	0.9543 ± 0.0023	0.9414 ± 0.0025
	0.9973 (3σ)	0.9952 ± 0.0007	0.9947 ± 0.0008
$D\pi^\pm$	0.6827 (1σ)	0.5945 ± 0.0053	0.5105 ± 0.0054
	0.9545 (2σ)	0.9391 ± 0.0026	0.9238 ± 0.0029
	0.9973 (3σ)	0.9960 ± 0.0007	0.9919 ± 0.0010
DK^\pm and $D\pi^\pm$	0.6827 (1σ)	0.6394 ± 0.0050	0.5839 ± 0.0051
	0.9545 (2σ)	0.9374 ± 0.0025	0.9112 ± 0.0030
	0.9973 (3σ)	0.9929 ± 0.0009	0.9912 ± 0.0010

For the two-body and four-body GLW/ADS analyses no information on systematic correlations is available. Consequently, they are assumed to be zero in the nominal combinations. Their possible influence is assessed by computing the effect of a large number of random correlation matrices on the expected confidence intervals. A maximum correlation of 75% is considered in the random matrices. The expected intervals are computed by generating pseudodatasets at the best-fit points of the three combinations, and then, for each pseudodataset, by computing its profile $\Delta\chi^2$ curve, and taking the average of these curves. The DK^\pm combination is unaffected. The $D\pi^\pm$ combination, however, is affected to a large extent, as the values of several observables are limited by systematic uncertainties. Conservatively, the maximum of the p -values observed for all random correlation matrices is considered. The nominal 1σ intervals are asymmetrically enlarged by 12% to match the maximum. The full combination is only slightly affected. The systematic uncertainty is fully concentrated in the lower side of the interval. Therefore, a systematic uncertainty of 2.5° (5.0°) is added in quadrature to the lower 1σ (2σ) errors.

The linearity of the combination procedure was checked by computing values for all observables using the best-fit point of the full combination and the relations from Section 2. Assuming the experimental covariances, the best-fit point was perfectly reproduced, and the procedure was found to be unbiased.

In summary, the DK^\pm combination does not require corrections. In case of the $D\pi^\pm$ and full combinations, the intervals are enlarged to account for both neglected systematic correlations and undercoverage.

6 Conclusion

A combination of recent LHCb results [23–25] is used to measure the CKM angle γ . The decays $B^\pm \rightarrow DK^\pm$ and $B^\pm \rightarrow D\pi^\pm$ are used, where the D meson decays into K^+K^- , $\pi^+\pi^-$, $K^\pm\pi^\mp$, $K_s^0\pi^+\pi^-$, $K_s^0K^+K^-$, or $K^\pm\pi^\mp\pi^+\pi^\mp$ final states. The effect of $D^0-\bar{D}^0$

mixing is taken into account in the ADS analysis of both $B^\pm \rightarrow DK^\pm$ and $B^\pm \rightarrow D\pi^\pm$ decays. Using only $B^\pm \rightarrow DK^\pm$ results, a best-fit value in $[0, 180]^\circ$ of $\gamma = 72.0^\circ$ is found and confidence intervals are set using a frequentist procedure

$$\begin{aligned}\gamma &\in [56.4, 86.7]^\circ \quad \text{at 68\% CL,} \\ \gamma &\in [42.6, 99.6]^\circ \quad \text{at 95\% CL.}\end{aligned}$$

Taking the best-fit value as central value, the first interval is translated to

$$\gamma = (72.0^{+14.7}_{-15.6})^\circ \text{ at 68\% CL.}$$

At 99% CL a second (local) minimum contributes to the interval. When combining results from $B^\pm \rightarrow D\pi^\pm$ decays alone, a best-fit value of $\gamma = 18.9^\circ$ is found and the following confidence intervals are set

$$\gamma \in [7.4, 99.2]^\circ \cup [167.9, 176.4]^\circ \quad \text{at 68\% CL,}$$

and no constraint is set at 95% CL. For the first time, information from $B^\pm \rightarrow D\pi^\pm$ decays is included in a combination. When these results are included, the best-fit value becomes $\gamma = 72.6^\circ$ and the following confidence intervals are set

$$\begin{aligned}\gamma &\in [55.4, 82.3]^\circ \quad \text{at 68\% CL,} \\ \gamma &\in [40.2, 92.7]^\circ \quad \text{at 95\% CL.}\end{aligned}$$

All quoted values are modulo 180° . The coverage of our frequentist method was evaluated and found to be exact when combining $B^\pm \rightarrow DK^\pm$ results alone, and accurate within 4% (2%) at 1σ (2σ) when combining $B^\pm \rightarrow DK^\pm$ and $B^\pm \rightarrow D\pi^\pm$ results. The final intervals have been scaled up to account for this undercoverage, and to account for neglected systematic correlations.

Acknowledgements

We express our gratitude to our colleagues in the CERN accelerator departments for the excellent performance of the LHC. We thank the technical and administrative staff at the LHCb institutes. We acknowledge support from CERN and from the national agencies: CAPES, CNPq, FAPERJ and FINEP (Brazil); NSFC (China); CNRS/IN2P3 and Region Auvergne (France); BMBF, DFG, HGF and MPG (Germany); SFI (Ireland); INFN (Italy); FOM and NWO (The Netherlands); SCSR (Poland); ANCS/IFA (Romania); MinES, Rosatom, RFBR and NRC ‘‘Kurchatov Institute’’ (Russia); MinECo, XuntaGal and GENCAT (Spain); SNSF and SER (Switzerland); NAS Ukraine (Ukraine); STFC (United Kingdom); NSF (USA). We also acknowledge the support received from the ERC under FP7. The Tier1 computing centres are supported by IN2P3 (France), KIT and BMBF (Germany), INFN (Italy), NWO and SURF (The Netherlands), PIC (Spain), GridPP (United Kingdom). We are thankful for the computing resources put at our disposal by Yandex LLC (Russia), as well as to the communities behind the multiple open source software packages that we depend on.

References

- [1] N. Cabibbo, *Unitary symmetry and leptonic decays*, Phys. Rev. Lett. **10** (1963) 531; M. Kobayashi and T. Maskawa, *CP violation in the renormalizable theory of weak interaction*, Prog. Theor. Phys. **49** (1973) 652.
- [2] J. Zupan, *The case for measuring γ precisely*, arXiv:1101.0134, presented at CKM2010, Warwick, UK, 6–10 Sep. 2010.
- [3] K. Trabelsi, *Study of direct CP in charmed B decays and measurement of the CKM angle γ at Belle*, arXiv:1301.2033, presented at CKM2012, Cincinnati, USA, 28. Sep.–2. Oct. 2012.
- [4] Babar collaboration, J. P. Lees *et al.*, *Observation of direct CP violation in the measurement of the Cabibbo-Kobayashi-Maskawa angle γ with $B^\pm \rightarrow D^{(*)}K^{(*)\pm}$ decays*, Phys. Rev. **D** (2013) 052015, arXiv:1301.1029.
- [5] CKMfitter group, J. Charles *et al.*, *CP violation and the CKM matrix: assessing the impact of the asymmetric B factories*, Eur. Phys. J. **C41** (2005) 1, arXiv:hep-ph/0406184, updated results and plots available at: <http://ckmfitter.in2p3.fr>, “ICHEP2012” result.
- [6] UTfit collaboration, M. Bona *et al.*, *The 2004 UTfit collaboration report on the status of the unitarity triangle in the standard model*, JHEP **07** (2005) 028, arXiv:hep-ph/0501199, updated results and plots available at: <http://www.utfit.org/UTfit/>, “Winter 2013 (pre-Moriond 13)” result.
- [7] M. Gronau and D. Wyler, *On determining a weak phase from CP asymmetries in charged B decays*, Phys. Lett. **B265** (1991) 172.
- [8] M. Gronau and D. London, *How to determine all the angles of the unitarity triangle from $B_d^0 \rightarrow DK_S$ and $B_s^0 \rightarrow D\phi$* , Phys. Lett. **B253** (1991) 483.
- [9] D. Atwood, I. Dunietz, and A. Soni, *Enhanced CP violation with $B \rightarrow KD^0(\bar{D}^0)$ modes and extraction of the CKM angle γ* , Phys. Rev. Lett. **78** (1997) 3257, arXiv:hep-ph/9612433.
- [10] D. Atwood, I. Dunietz, and A. Soni, *Improved methods for observing CP violation in $B^\pm \rightarrow KD$ and measuring the CKM phase γ* , Phys. Rev. **D63** (2001) 036005, arXiv:hep-ph/0008090.
- [11] A. Giri, Y. Grossman, A. Soffer, and J. Zupan, *Determining γ using $B^\pm \rightarrow DK^\pm$ with multibody D decays*, Phys. Rev. **D68** (2003) 054018, arXiv:hep-ph/0303187.
- [12] CLEO collaboration, N. Lowrey *et al.*, *Determination of the $D^0 \rightarrow K^-\pi^+\pi^0$ and $D^0 \rightarrow K^-\pi^+\pi^+\pi^-$ coherence factors and average strong-phase differences using quantum-correlated measurements*, Phys. Rev. **D80** (2009) 031105, arXiv:0903.4853, “mixing constrained” result.

- [13] J. P. Silva and A. Soffer, *Impact of $D^0-\bar{D}^0$ mixing on the experimental determination of γ* , Phys. Rev. **D61** (2000) 112001, arXiv:hep-ph/9912242.
- [14] Y. Grossman, A. Soffer, and J. Zupan, *The effect of $D-\bar{D}$ mixing on the measurement of γ in $B \rightarrow DK$ decays*, Phys. Rev. **D72** (2005) 031501, arXiv:hep-ph/0505270.
- [15] A. Bondar, A. Poluektov, and V. Vorobiev, *Charm mixing in the model-independent analysis of correlated $D^0\bar{D}^0$ decays*, Phys. Rev. **D82** (2010) 034033, arXiv:1004.2350.
- [16] M. Rama, *Effect of $D-\bar{D}$ mixing in the extraction of γ with $B^- \rightarrow D^0 K^-$ and $B^- \rightarrow D^0 \pi^-$ decays*, arXiv:1307.4384.
- [17] LHCb collaboration, R. Aaij *et al.*, *Observation of $D^0-\bar{D}^0$ oscillations*, Phys. Rev. Lett. **110** (2012) 101802, arXiv:1211.1230.
- [18] LHCb collaboration, R. Aaij *et al.*, *Search for direct CP violation in $D^0 \rightarrow h^- h^+$ modes using semileptonic B decays*, arXiv:1303.2614.
- [19] LHCb collaboration, *A search for time-integrated CP violation in $D^0 \rightarrow K^- K^+$ and $D^0 \rightarrow \pi^- \pi^+$ decays*, LHCb-CONF-2013-003.
- [20] M. Martone and J. Zupan, *$B^\pm \rightarrow DK^\pm$ with direct CP violation in charm*, Phys. Rev. **D87** (2013) 034005, arXiv:1212.0165.
- [21] B. Bhattacharya, D. London, M. Gronau, and J. L. Rosner, *Shift in weak phase γ due to CP asymmetries in D decays to two pseudoscalar mesons*, Phys. Rev. **D87** (2013) 074002, arXiv:1301.5631.
- [22] W. Wang, *CP violation effects on the measurement of γ from $B \rightarrow DK$* , Phys. Rev. Lett. **110** (2013) 061802, arXiv:1211.4539.
- [23] LHCb collaboration, R. Aaij *et al.*, *A model-independent Dalitz plot analysis of $B^\pm \rightarrow DK^\pm$ with $D \rightarrow K_S^0 h^+ h^-$ ($h = \pi, K$) decays and constraints on the CKM angle γ* , Phys. Lett. **B718** (2012) 43, arXiv:1209.5869.
- [24] LHCb collaboration, R. Aaij *et al.*, *Observation of CP violation in $B^\pm \rightarrow DK^\pm$ decays*, Phys. Lett. **B712** (2012) 203, arXiv:1203.3662.
- [25] LHCb collaboration, R. Aaij *et al.*, *Observation of the suppressed ADS modes $B^\pm \rightarrow [\pi^\pm K^\mp \pi^+ \pi^-]_D K^\pm$ and $B^\pm \rightarrow [\pi^\pm K^\mp \pi^+ \pi^-]_D \pi^\pm$* , Physics Letters **B** (2013) 44, arXiv:1303.4646.
- [26] Heavy Flavor Averaging Group, Y. Amhis *et al.*, *Averages of b-hadron, c-hadron, and τ -lepton properties as of early 2012*, arXiv:1207.1158, updates available online at <http://www.slac.stanford.edu/xorg/hfag>, “allowing all CP violation” result.

- [27] CLEO collaboration, R. A. Briere *et al.*, *First model-independent determination of the relative strong phase between D^0 and $\bar{D}^0 \rightarrow K_S^0 \pi^+ \pi^-$ and its impact on the CKM angle $\gamma/\phi(3)$ measurement*, Phys. Rev. **D80** (2009) 032002, [arXiv:0903.1681](#).
- [28] Likelihood profile provided by J. Libby.
- [29] B. Sen, M. Walker, and M. Woodroofe, *On the unified method with nuisance parameters*, Statistica Sinica **19** (2009) 301.
- [30] R. Fleischer, N. Serra, and N. Tuning, *Tests of factorization and $SU(3)$ relations in B decays into heavy-light final states*, Phys. Rev. **D83** (2011) 014017, [arXiv:1012.2784](#).
- [31] R. L. Berger and D. D. Boos, *P-values maximized over a confidence set for the nuisance parameter*, J. Amer. Statist. Assoc. **89** (1994) 1012.

7 Supplemental material

The following material is to be made publicly available, but is not to be included in the paper.

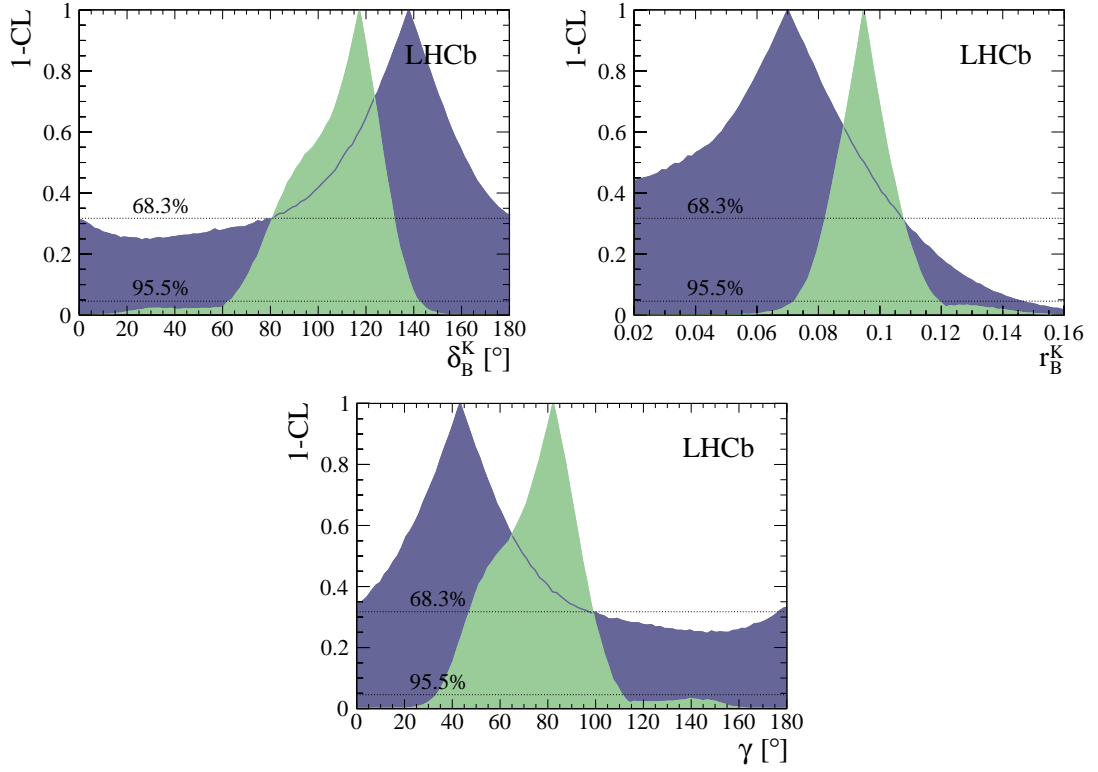


Figure 5: Graphs showing $1 - \text{CL}$ for δ_B^K , r_B^K , and γ , separately for the GLW/ADS (light green) and GGSZ (dark purple) parts of the DK^\pm -only combination.

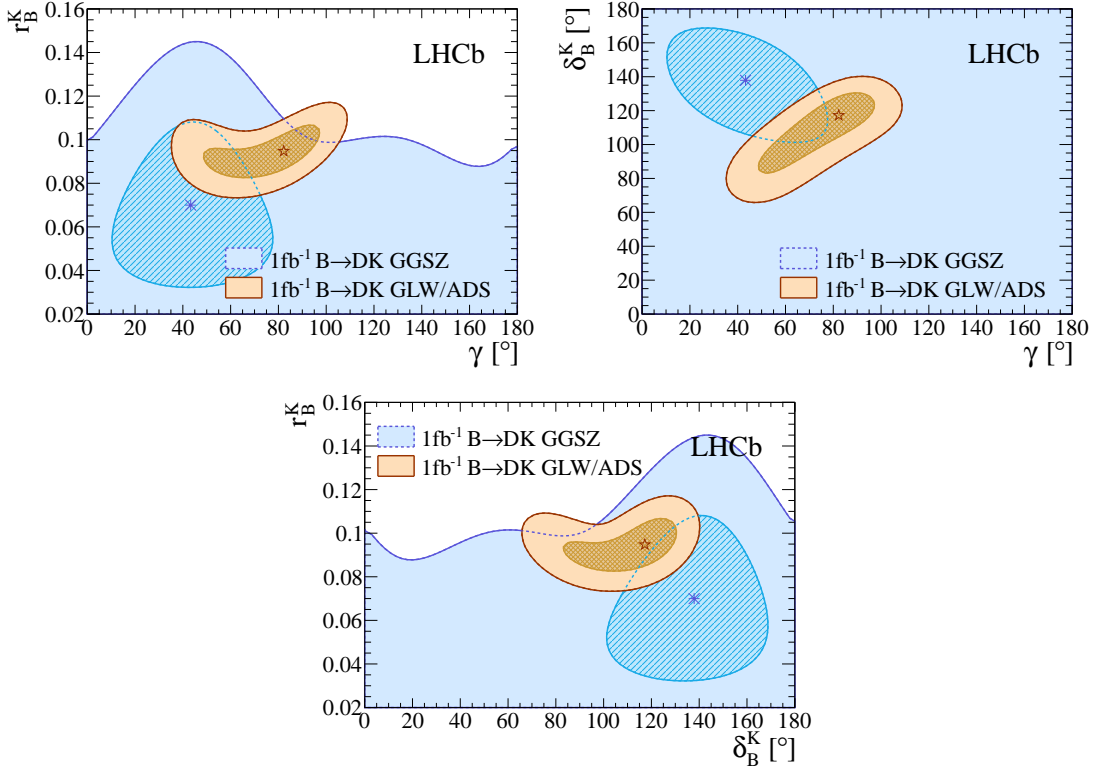


Figure 6: Profile likelihood contours, separately for the GGSZ (blue) and two-body and four-body GLW/ADS (orange) parts of the DK^\pm only combination. The contours are the usual $n\sigma$ profile likelihood contours, where $\Delta\chi^2 = n^2$ with $n = 1, 2$. The markers correspond to the best-fit points.

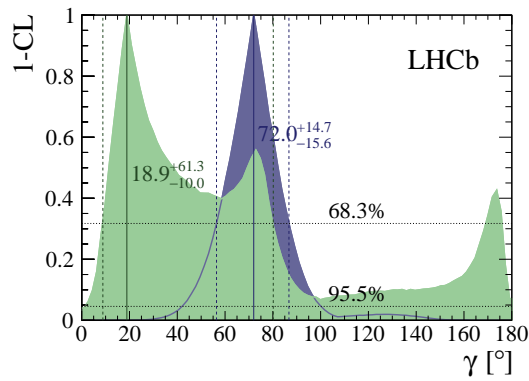


Figure 7: Graphs showing $1 - \text{CL}$ for γ , separately for the DK^\pm -only combination (dark purple) and $D\pi^\pm$ -only combination (light green).